Abstract—The larvae of marine fishes often differ substantially in appearance from their adult forms. While sometimes visually striking, these larvae can be difficult to identify. Cusk-eels of the predominantly deep-sea family Ophidiidae have epipelagic larval stages that are remarkably diverse in appearance and some of these larvae, such as the bony-eared assfish (*Acanthonus armatus*), are widely popular subjects for blackwater photographers. Recently, a larva was photographed and collected off the east coast of Florida that resembled a bony-eared assfish but differed in pectoral-fin morphology. Based on counts and DNA data, we identified this larva as the gargoyle cusk (*Xyelacyba myersi*), a species for which the larval stage has yet to be described. With an improved understanding of cusk-eel larval morphology, we found and identified a single larval specimen of the spiny blind brotulid (*Tauredophidium hextii*) collected from the eastern Indian Ocean in 1977, another species for which the larval stage has yet to be described. We describe these novel larvae, compare them to a newly caught larval *Acanthonus* from Hawaii, and highlight morphological similarities and differences among them. Previous works have suggested a close relationship among the monotypic genera *Acanthonus, Tauredophidium,* and *Xyelacyba,* and we found 4 larval and 6 adult shared morphological traits, including an opercular-spine locking mechanism, that support these taxa forming a clade. Considering these findings and that more than a third of ophidiid genera are monotypic, we modify the classification of these 3 taxa so they are classified in the same genus, *Acanthonus,* to highlight their relatedness. Our study demonstrates the scientific importance of images and specimens collected by blackwater divers for species identification and further highlights their significance in understanding evolutionary relationships.

Discovery and description of elaborate larval cusk-eels and the relationships among *Acanthonus, Tauredophidium,* and *Xyelacyba* (Teleostei: Ophidiidae)

Matthew G. Girard (contact author)[1,2]
Ai Nonaka[1]
Carole C. Baldwin[1]
G. David Johnson[1]

Email address for contact author: GirardMG@si.edu

[1] Department of Vertebrate Zoology
National Museum of Natural History
Smithsonian Institution
10th and Constitution Avenue NW
Washington, D.C. 20560

[2] Biodiversity Institute
University of Kansas
1345 Jayhawk Boulevard
Lawrence, Kansas 66045

Introduction

> *The angel from Heaven has arrived as a larval fish*
> —Geoff Moser in an email about blackwater photos of the bony-eared assfish (*Acanthonus armatus*)

Many marine fish larvae possess dazzling features and are strikingly different in overall appearance from their adult forms (Moser, 1981). With eyes on elongated stalks (e.g., Weihs and Moser, 1981; Kawaguchi and Moser, 1984), conspicuous head spines (e.g., Johnson, 1984, 1988), external guts (e.g., Fraser and Smith, 1974), globes of tissue surrounding their bodies (e.g., Pietsch, 1984), and, very commonly, elongated, ornamented fin rays (e.g., Johnson and Washington, 1987; Baldwin et al., 1991; Fahay and Nielsen, 2003), these prominent larval traits are usually limited to early pelagic ontogenetic stages, becoming reduced or integrated into other features in adults. Linking the larval and adult stages of marine species can thus be difficult, and historically, some larvae have been classified as different species or even different families than their adult counterparts (as discussed by Johnson, 1988; Tyler et al., 1989; Johnson and Bertelsen, 1991; Winterbottom, 1993; Baldwin and Johnson, 1995; Johnson et al., 2009). Counts of fin rays and myomeres, among other traits, have allowed researchers to describe the larvae of thousands of species (e.g., Moser et al., 1984; Okiyama, 1988; Moser, 1996; Leis and Carson-Ewart, 2000; Richards, 2005; Fahay, 2007; Okiyama, 2014; Leis, 2015). Further, DNA barcoding efforts (e.g., Weigt et al., 2012; Baldwin and Johnson, 2014; Nonaka et al., 2021; Girard et al., 2023a, 2023b) are substantially aiding these linking efforts and helping researchers identify new larval forms not yet known to science.

Cusk-eels (Ophidiidae) are a family of approximately 280 species in 50 genera (Fricke et al., 2022) and represent some of the deepest-dwelling vertebrates on Earth (Gerringer et al., 2021). Although the adult forms are generally similar in appearance, cusk-eel larvae are remarkably diverse, with some having external or "exterilium" guts (e.g., Fraser and Smith, 1974); elongate dorsal-, anal-, pectoral-, and pelvic-fin rays (e.g., Fahay and Nielsen, 2003); or trailing dermal filaments (e.g., Okiyama and Yamaguchi, 2004). These larval morphologies have been used to propose evolutionary relationships, such as the hypothesized sister-group relationship between *Brotulotaenia* Parr, 1933 and *Lamprogrammus* Alcock, 1891 (Wood-Mason

and Alcock, 1891; Parr, 1933; Fahay and Nielsen, 2003). However, many ophidiid larvae remain unknown or unidentified (e.g., Okiyama, 1988, 2014), limiting the utility of larval traits for informing evolutionary relationships among cusk-eels.

The gargoyle cusk (*Xyelacyba myersi* Cohen, 1961) is a demersal cusk-eel found along the continental slope of tropical and subtropical seas (Cohen, 1961; Nielsen et al., 1999; Fig. 1A). Belonging to a monotypic genus, adults are easily differentiated from other cusk-eels by their massive heads and prominent spines on the opercle and preopercle. Only a few species of cusk-eels have similar head spination, including the bony-eared assfish (*Acanthonus armatus* Günther, 1878) and the spiny blind brotulid (*Tauredophidium hextii* Alcock, 1890; Fig. 1, B and C). In his description of *X. myersi*, Cohen (1961:288) noted that it is "apparently nearest" to *A. armatus* and *T. hextii* based on overall similarity. These 3 taxa were subsequently placed in the Neobythitinae tribe Sirembini (Cohen and Nielsen, 1978) along with *Dannevigia* Whitley, 1941, *Hoplobrotula* Gill, 1863, and *Sirembo* Bleeker, 1857 (Bleeker, 1857; Gill, 1863; Whitley, 1941). Later, Howes (1992) described the anatomy of *A. armatus*, highlighting several additional anatomical similarities among *Acanthonus* Günther, 1878, *Tauredophidium* Alcock, 1890, and *Xyelacyba* Cohen, 1961, including an expanded *dilatator operculi* and the presence of a distinct preopercular–opercular ligament (Günther, 1878; Alcock, 1890; Cohen, 1961). However, Howes (1992:130) could not resolve the relationships among these taxa, as the anatomies of *T. hextii* and *X. myersi* were "too imperfectly known." Among *Acanthonus, Tauredophidium,* and *Xyelacyba,* only the larval form of *A. armatus* has been described (Fig. 2A). Okiyama (1981) described a single 47.6 mm standard length (SL) specimen from the surface waters of Iriomote Island, Japan, with elongate upper pectoral-fin rays. This unusual morphology among larval ophidiids was linked to *A. armatus* in a brief description by Okiyama (1981). Later, Okiyama (2014) described the larva as having the dorsalmost 3 to 5 pectoral-fin rays extremely long, with the longest almost equal to SL. With the recent popularity of blackwater diving and photography (see Nonaka et al., 2021), this elaborate larva has been a widely sought-after target among blackwater photographers (Fig. 2A). However, larval morphology of the putative sister taxa of *A. armatus* (i.e., *X. myersi* and *T. hextii*) remain unknown.

During blackwater dives off the eastern Florida coast in September 2020, divers photographed and captured a larva with elongate and orange-to-yellow pectoral-fin rays. The larva was initially identified as *A. armatus* due to the elongate upper pectoral-fin rays known to occur in this taxon (see Okiyama, 2014). However, the lower pectoral-fin rays become gradually longer and lack distal membranes in this larva (Fig. 2B), differing notably from those described for larval *A. armatus*. Based on count and measurement data, along with DNA barcodes from this specimen and newly collected larval *A. armatus* from blackwater dives off the coast of Hawaii, we identified the Florida specimen as the larva of *X. myersi*. With an improved understanding of larval *Acanthonus* and *Xyelacyba* morphology, we examined historical larval collections and discovered a single larva of *T. hextii* from a 1977 survey by The National Research Institute of Far Seas Fisheries in the eastern Indian Ocean. Herein, we describe these novel larvae and provide a revised description of larval *A. armatus*. Given the overall similarity among these 3 larvae and the previous work by Cohen (1961), Cohen and Nielsen (1978), and Howes (1992) suggesting a close relationship among *A. armatus, T. hextii,* and *X. myersi,* we then examined the adult morphology of these 3 taxa using a combination of ethanol, cleared-and-stained, and micro-computed-tomography-scanned (μCT) specimens, highlight shared morphological traits, and hypothesize relationships among them.

Materials and methods

In-situ imaging and capture of larval specimens

Larval specimens of *A. armatus* and *X. myersi* used in this study were caught during nighttime drift-based scuba dives in the epipelagic realm over deep-water environments, also known as blackwater diving (see Nonaka et al., 2021 for more information). Each specimen was photographed in situ using a Nikon D500 camera (Nikon Inc., Tokyo, Japan) with a 60 mm macro lens within a waterproof housing, two 2000-lumen focus lights, and 2 Ikelite DS160 strobes (Ikelite, Indianapolis, IN). Each photographed fish was then captured using a vessel filled with sea water. Following the dive, the specimen was transferred into a solution of laboratory grade 95% ethanol (see Nonaka et al., 2021). All methods of capture and preservation conform to the *Guidelines for the Use of Fishes in Research* established by the American Fisheries Society, American Institute of Fishery Research Biologists, and American Society of Ichthyologists and Herpetologists (Jenkins et al., 2014). Larvae collected off West Palm Beach were acquired under Florida permit SAL-21-2155A-SR.

Morphological examination and laboratory imaging of larvae and adults

Measurements of preserved specimens were taken with a digital caliper to the nearest 0.1 mm. External and internal morphology were examined in larval and adult specimens that were in ethanol, cleared and stained, and/or scanned using a μCT. Cleared-and-stained

Figure 1

Adult (**A**) gargoyle cusk (*Xyelacyba myersi*) (USNM 407808, 164 mm standard length [SL]), (**B**) bony-eared assfish (*Acanthonus armatus*) (UF 180163, 122 mm SL), and (**C**) spiny blind brotulid (*Tauredophidium hextii*) (BMNH 1992.2.4.3-4, 104 mm SL). Scale bars=1 cm.

specimens were prepared following Potthoff (1984) with the modifications listed in Girard et al. (2020). Whole or stained specimens were examined with a Nikon SMZ-745T microscope (Nikon Inc.). We documented morphological features using the camera, lens, focus stacking rail, software, and lighting described in Girard et al. (2020) or a SwiftCam SC2003R-FL microscope camera (Swift Optical Instruments Inc., Schertz, TX). As not all species could be cleared and stained due to their rarity in museum collections, we also used µCT scanning to view internal osteology. Specimens were scanned using a GE Phoenix v|tome|x M240/180kV Dual Tube µCT (Waygate Technologies, Wunstorf, Germany) at the National Museum of Natural History, Smithsonian Institution (NMNH) using 60 kV, 400 µA, an exposure time of 250 ms, and a voxel size of 54.9 µm. The resulting image stacks were reconstructed into a 3-dimensional image using the software package datos|x reconstruction vers. 2.4.0 (Waygate Technologies). In addition to these newly scanned specimens, image stacks of other ophidiid species were downloaded from MorphoSource (available from www.morphosource.org, accessed March 2022) for examination and comparison. Specimen catalog numbers, preparation types, and MorphoSource media identifiers for all µCT-scanned specimens can be found in the Material examined section. The resulting isolated specimen image stacks were viewed and segmented via the

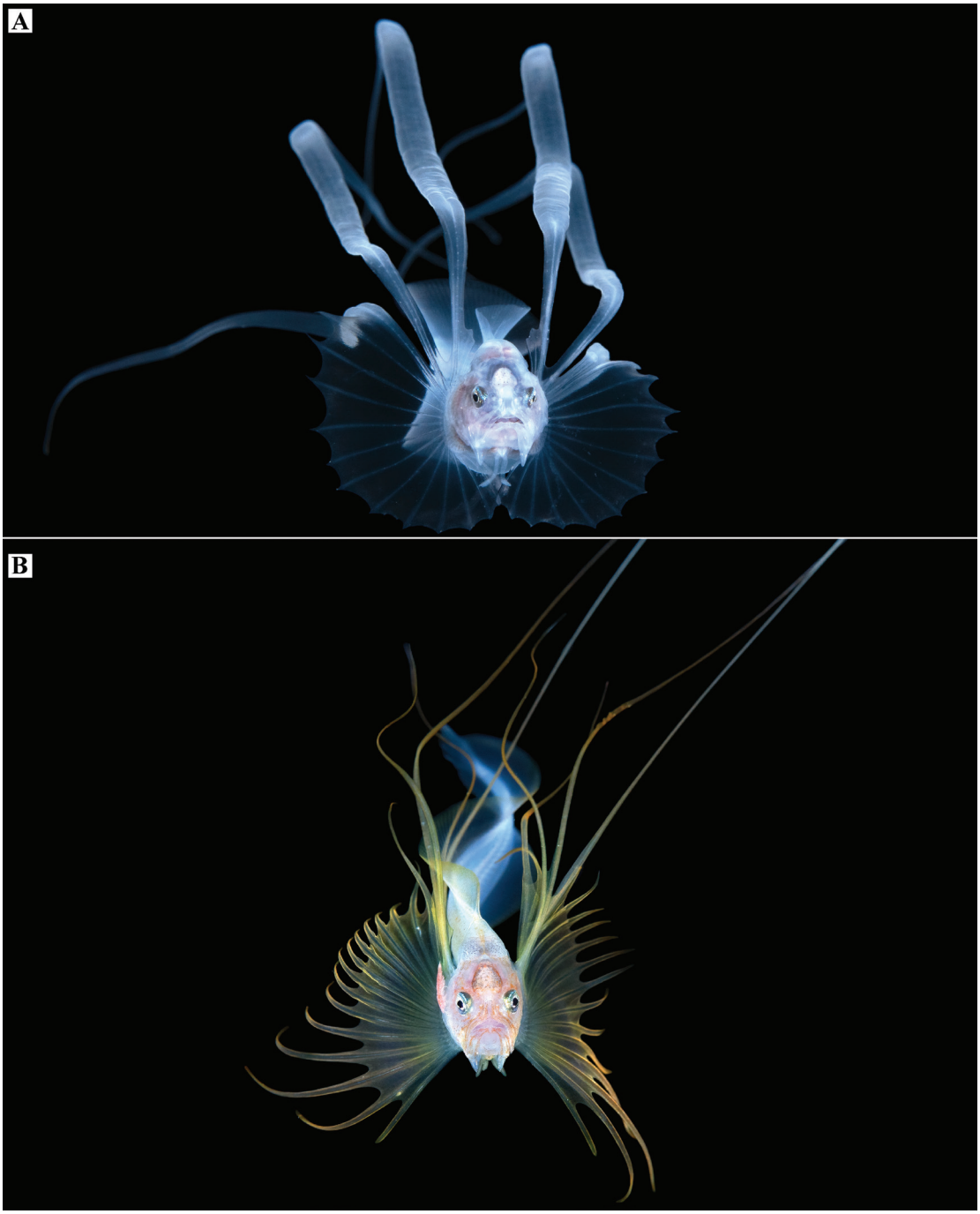

Figure 2

Blackwater photos of larval (**A**) bony-eared assfish (*Acanthonus armatus*) and (**B**) gargoyle cusk (*Xyelacyba myersi*) highlighting the differences in form and coloration of pectoral-fin rays. Photos were taken in the waters off West Palm Beach, Florida (**A**) the night of 29 May 2020 and (**B**) the night of 5 June 2020. Photos © Steven Kovacs.

Table 1

Voucher information, Barcode of Life Database (BOLD) Process ID numbers, and GenBank accession numbers for DNA sequences of larval and adult specimens used in this study.

	Voucher for molecular dataset	Developmental stage of voucher	Tissue for molecular dataset	GenBank accession number	BOLD accession number
Bythitidae					
Brosmophycis marginata	UW 47680	Adult	See voucher	JQ354026	FMV070-08
Cataetyx rubrirostris	UW 119892	Adult	See voucher	JQ354034	FMV486-11
Ophidiidae					
Acanthonus armatus	ASIZ P 802285	Adult	See voucher	KU943162	ZOSKT2012-16
Acanthonus armatus	CSIRO H.8139-04	Adult	CSIRO BW-A14287	Unavailable	FOAO1089-18
Acanthonus armatus	USNM 454556	Larva	See voucher	OP347161	XAT001-22
Acanthonus myersi	ASIZ P 801557	Adult	See voucher	KU885676	ZOSKT1556-16
Acanthonus myersi	ECO-CH-LP 6268	Larva	See voucher	Unavailable	MFLE343-13
Acanthonus myersi	USNM 464023	Larva	See voucher	OP347162	XAT002-22
Dicrolene filamentosa	USNM 422422	Adult	See voucher	MF956679	MOP074-12
Dicrolene tristis	ASIZ P 806598	Adult	See voucher	KU943170	ZOSKT342-16
Hoplobrotula armata	CSIRO H.7136.11	Adult	CSIRO BW-A10750	Unavailable	FOAM787-11
Hoplobrotula gnathopus	SAIAB ADC09-96.13	Adult	See voucher	GU804901	DSFSF748-09
Lamprogrammus brunswigi	ARC 28413	Adult	See voucher	KY033653	SCAFB1174-09
Lamprogrammus niger	USNM 435786	Adult	See voucher	MF956747	MOP706-12
Sirembo jerdoni	CSIRO H.6915-04	Adult	CSIRO BW-A8581	HQ956394	FOAL724-10
Sirembo metachroma	CSIRO H.7266-14	Adult	CSIRO BW-A11888	Unavailable	FOAN1095-11

SlicerMorph module (Rolfe et al., 2021) in 3D Slicer, vers. 4.13.0 (Fedorov et al., 2012). Methods for segmenting scanned specimens follow Girard et al. (2022).

DNA extraction and amplification

Extraction of genomic DNA was performed using a DNeasy tissue extraction kit (Qiagen, Germantown, MD) or a Gene Prep fully automated DNA extraction system (AutoGen, Holliston, MA) following the manufacturer's protocols. Protocols for tissue sampling, polymerase chain reaction, and sequencing cytochrome oxidase subunit 1 (COI) follow the methods described in Nonaka et al. (2021) and Weigt et al. (2012) using primers from Baldwin et al. (2009). Sequence contigs were built using Geneious, vers. 11.1.5 (Kearse et al., 2012) from DNA sequences of the complementary heavy and light strands. Sequences were edited in Geneious and assembled into FASTA files. Sequences have been deposited in both the GenBank database of the National Center for Biotechnology Information (available from https://www.ncbi.nlm.nih.gov/genbank/) and the Barcode of Life Database (available from http://www.boldsystems.org), with accession and process ID numbers for the respective databases listed in Table 1.

Taxon identification and analyses of molecular data

To verify taxon identity and generate a hypothesis of relationships for the newly sequenced taxa within a broader context of the Neobythitinae (*sensu* Cohen and Nielsen, 1978), we downloaded 14 COI sequences from members of the genera *Acanthonus, Brosmophycis* Gill, 1861, *Cataetyx* Günther, 1887, *Dicrolene* Goode and Bean, 1883, *Hoplobrotula, Lamprogrammus, Sirembo,* and *Xyelacyba* (Gill, 1861; Goode and Bean, 1883; Günther, 1887). Publicly available sequences of larval and adult *Acanthonus* and *Xyelacyba* were included to verify the identity of the newly sequenced specimens. The remaining taxa included represent genera previously hypothesized to be close allies of *Acanthonus, Tauredophidium,* and/or *Xyelacyba*. Downloaded sequences come from a series of published and unpublished works, including Chang et al. (2017), Kenchington et al. (2017), and Robertson et al. (2017; Table 1). Analyses were rooted on the red brotula (*Brosmophycis marginata*). A complete list of sampled taxa and sequence accession numbers can be found in Table 1, with catalog codes following Sabaj (2020). These sequences were collated into a single file with newly sequenced loci and aligned with MAFFT, vers. 7 (Katoh and Standley, 2013) within Geneious and exported as a phylip-format file for phylogenetic analyses. The aligned matrix, which was 652 bps in length (~96% complete) and contained 215 parsimony-informative sites, was broken into 3 partitions, one for each of the 3 codon positions in the protein-coding locus. These 3 partitions were input for ModelFinder function within IQ-Tree, vers. 2.1.3 (i.e., –MPF+MERGE; Chernomor et al., 2016; Kalyaanamoorthy et al., 2017; Minh et al., 2020), which selected the following partitioning scheme and models based on Bayesian information criterion: partition 1—TN+F+R2; partition 2+3—TIM2e+I. Phylogenetic analy-

sis was performed by 10 independent executions of IQ-Tree with the number of unsuccessful iterations to stop (-nstop) set to 2000. Support for the best-fitting topology of the dataset was generated using 200 standard bootstrap replicates (-bc) and reconciled with the most likely phylogeny using IQ-Tree (-con).

Results

Molecular analyses

The hypothesis of relationships recovered from our analysis of COI is shown in Figure 3A and has a score of –3473.439. The bootstrap values yielded 8 nodes (of 13 possible, ~61%) with a value of ≥80% and 5 nodes (~38%) with a value of ≥95% (Fig. 3A). The resulting topology verifies the identity of the newly captured larval specimens, as they are recovered in clades with samples from adult representatives. *Acanthonus* and *Xyelacyba* are recovered as reciprocally monophyletic and sister groups. This clade of *Acanthonus* and *Xyelacyba* is the sister group of a clade that includes reciprocally monophyletic groups of *Dicrolene, Hoplobrotula, Lamprogrammus,* and *Sirembo*.

Taxonomic changes to the genera *Acanthonus, Tauredophidium*, and *Xyelacyba*

Based on the morphological characters we discuss below (Fig. 3B), as well as a limited sampling of DNA-based characters, we synonymize the genera *Tauredophidium* and *Xyelacyba* with the genus *Acanthonus*. A diagnosis for the revised genus is as follows:

Acanthonus Günther 1878
Type species: *Acanthonus armatus* Günther, 1878
Species included: *Acanthonus armatus* Günther, 1878, *A. hextii* (Alcock, 1890), *A. myersi* (Cohen, 1961).

Diagnosis

The genus *Acanthonus* is distinguished from all other ophidiiform genera by the following combination of larval and adult characters: Larvae—(1) pectoral-fin base broad; (2) multiple pectoral-fin rays elongate and free; (3) gut rotund; (4) dense melanophores surrounding gut. Adults—(5) opercular and preopercular spines with longitudinal keel; (6) posterodorsal process of the quadrate broad, embracing preopercle; (7) posterodorsal process distantly spaced and gap between preopercle and quadrate; (8) symplectic with posterior spur; (9) opercular spine-extending and locking mechanism; (10) laterally flared frontal (Fig. 3B).

Remarks

The genus is referred to as thorny assfishes to highlight the prominent opercular and preopercular spines.

Detailed character information is provided in the Discussion section. Hereafter, we treat the genus *Acanthonus* as including the 3 species listed above.

In-situ observations of larval thorny assfishes

The following observation data were provided by S. Kovacs[1]: Larvae of both *A. armatus* and *A. myersi* are exceedingly rare, with *A. armatus* seen twice and *A. myersi* seen 3 times in 800–1000 dives over an 8-to-9-year timespan. The larva of *A. armatus* was seen only once over the course of 90 dives in Kona, Hawaii (2021). Both larvae behaved similarly, swimming slowly, side to side, for several centimeters before turning to change direction. One large individual of *A. armatus* added short bursts of accelerated swimming every 5–10 minutes over an hour-long period. Both larvae were seemingly unfazed by camera flashes and continued to swim slowly back and forth, with some individuals swimming toward the light and camera.

Description of larval *Acanthonus myersi*

Postflexion specimen (USNM 464023) collected at a depth of ~15 m over a bottom depth of ~200 m, ~10 km offshore of West Palm Beach, Florida, the night of 3 September 2020 by S. Kovacs; photographed by S. Kovacs. Measurements and counts: SL 13.6 mm; total length (TL) 14.7 mm; dorsal-fin rays 87; anal-fin rays 75; pectoral-fin rays 20; pelvic-fin rays 2; caudal-fin rays 9; precaudal vertebrae 12 (Fig. 4). Proportions in SL: preanal length (snout to anterior end of anus) 40.2%; head length (HL) 20.5%; depth of pectoral-fin base 15.7%; length of lateral pelvic-fin ray 24.5%; length of medial pelvic-fin ray 28.9%; caudal peduncle absent, narrowest caudal depth (at caudal-fin base) 3.3%; caudal-fin length 8.7% (Table 2). Proportions in HL: dorsal fin origin 128.6%; snout length 27.2%; eye diameter 23.3%; postorbital length 46.4%; upper jaw length 53.2%; lower jaw length 50.9%; lower jaw width 12.6% (Table 2).

The head is large, deeper than long, and the body tapers posteriorly to the caudal fin. Maxilla and premaxilla are present, and the supramaxilla is indistinguishable. The distal end of the maxilla dorsoventrally expands with the concave posterior margin. The posterior tip of the premaxilla nearly reaches the posterior margin of the maxilla. A large rostral cartilage is attached to the ascending process of the premaxilla. The premaxilla and dentary have small, distantly spaced teeth. The opercular series has no spines. Eight branchiostegals are evident (full complement). The body and head are scaleless. The pectoral fin is large and fan-like, with a broad base. There are 20 pectoral-fin rays on each side, and the

[1] Kovacs, S. 2022. Personal commun. Blackwater photographer, West Palm Beach, FL.

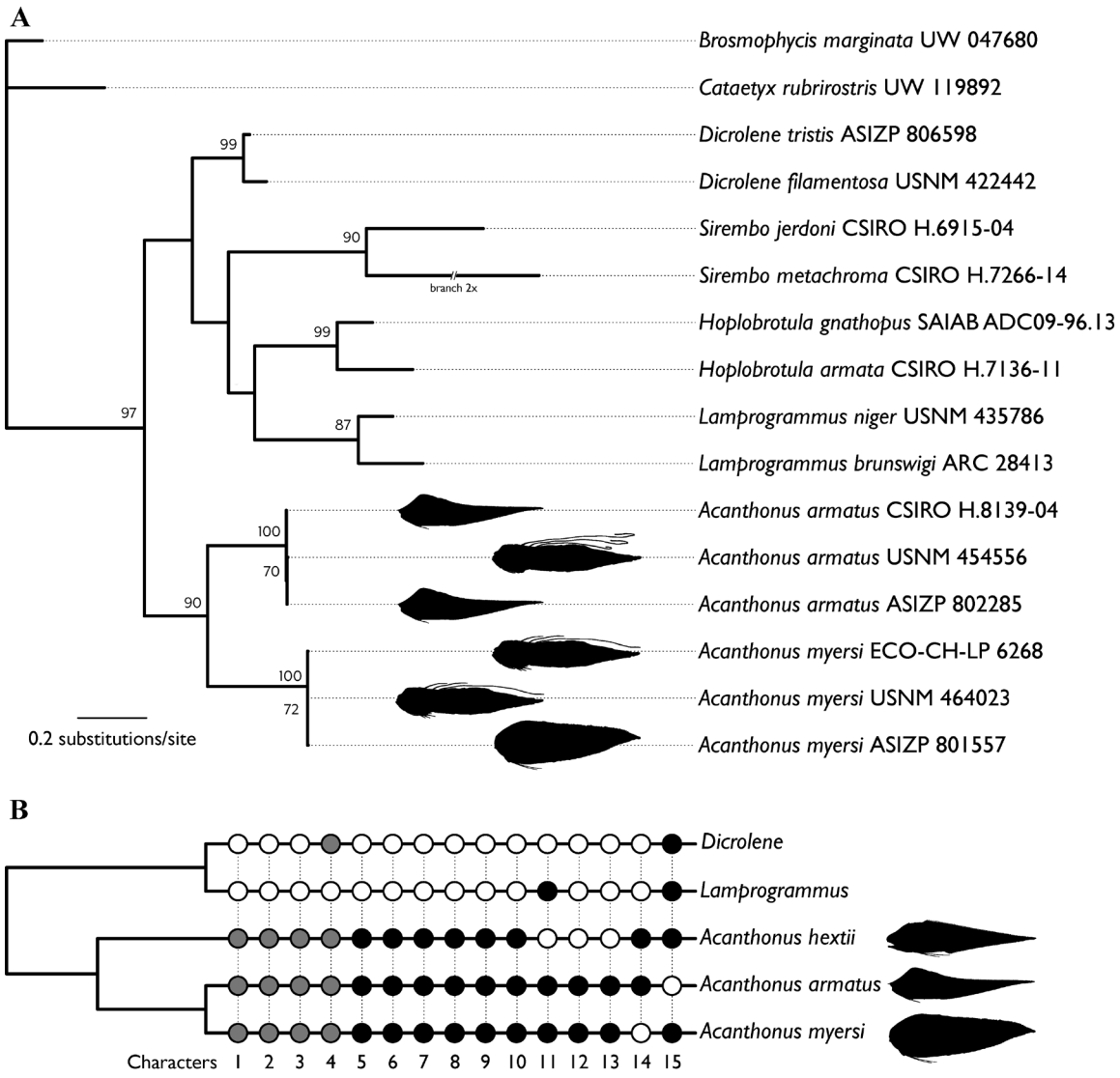

Figure 3

(**A**) Hypotheses of relationships from partitioned likelihood analysis of *Acanthonus* larvae, adults, and outgroup taxa based on cytochrome oxidase subunit 1 (COI) sequences. Support was determined based on 200 bootstrap replicates. Clades with 70% or higher bootstrap support are noted on the nodes with their bootstrap percentage. Branch leading to *Sirembo metachroma* is reduced in length by half. Silhouettes corresponding with terminals of *Acanthonus* show the developmental stage of the tissue voucher (i.e., larvae with elongate pectoral-fin rays or adult). (**B**) Distribution of larval and adult characters based on proposed relationships between species of *Acanthonus*. White circles represent the absence of the character state. Gray circles represent the presence of a larval character state. Black circles represent the presence of an adult character state. Characters: (1) pectoral-fin base broad; (2) multiple pectoral-fin rays elongate and free; (3) gut rotund; (4) dense melanophores surrounding gut; (5) opercular and preopercular spines with longitudinal keel; (6) posterodorsal process of the quadrate broad, embracing preopercle; (7) posterodorsal process distantly spaced and gap between preopercle and quadrate; (8) symplectic with posterior spur; (9) opercular spine-extending and locking mechanism; (10) laterally flared frontal; (11) cancellous bone; (12) confluence of palatine and vomerine tooth plates; (13) tripartite pharyngobranchial one; (14) ethmoid prong; (15) sphenotic expanded laterally.

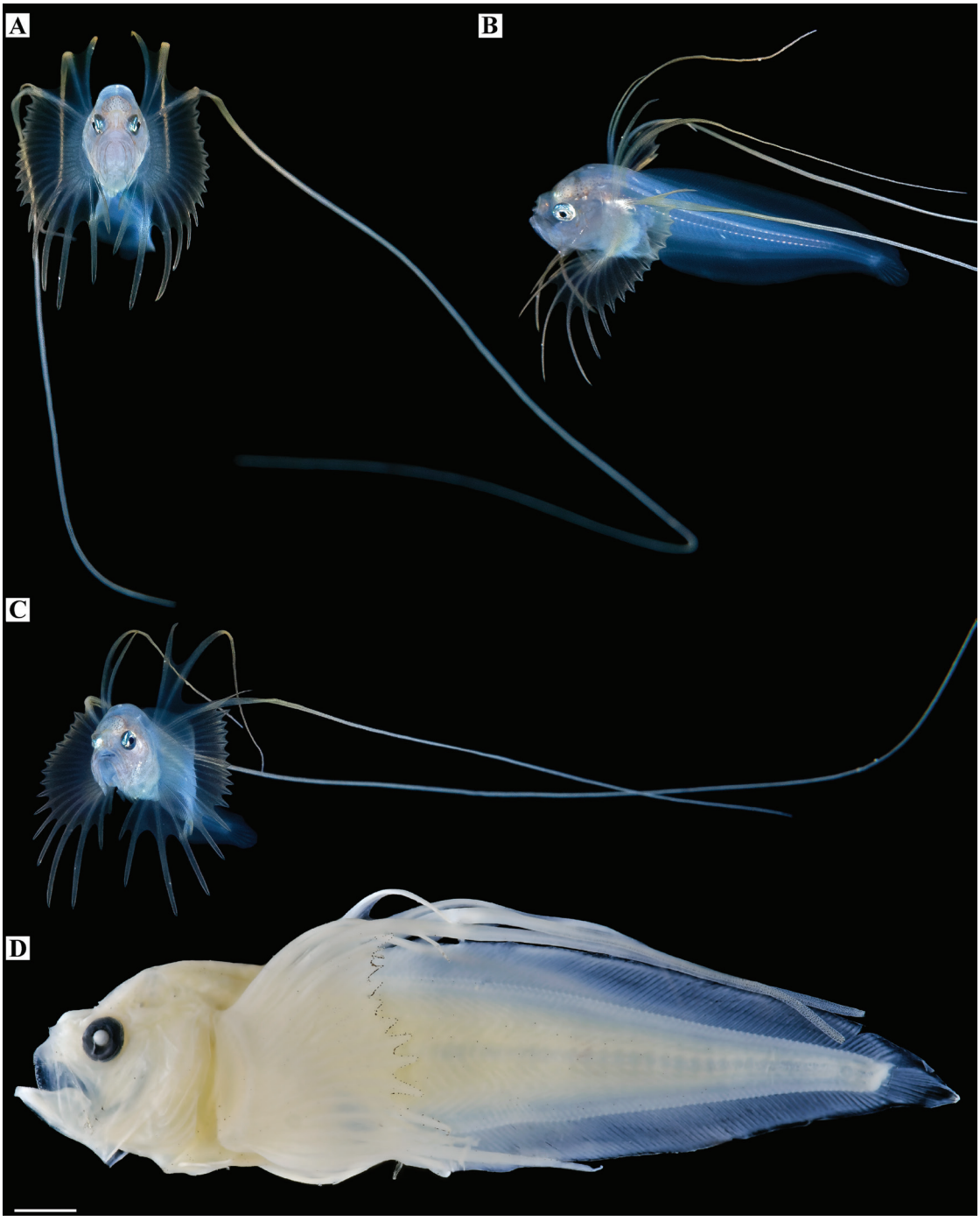

Figure 4

(**A–C**) Blackwater photos of a larval gargoyle cusk (*Acanthonus myersi*) (USNM 464023, 13.6 mm standard length) in the postflexion stage taken in the waters off West Palm Beach, Florida, on the night of 3 September 2020. Photos © Steven Kovacs. (**D**) Preserved specimen USNM 464023. Scale bar=1 mm.

membrane between each ray is truncated distally, leaving the tip of each ray free from the membrane for half or more of its length (Figs. 2B, 4A–C). In-situ images of fixed specimen and other uncollected specimens show the elongate rays were damaged and truncated during capture and subsequent fixation (compare Figs. 2B and 4A–C with 4D). Accordingly, the TL of the elongate rays is not reported. Pelvic-fin rays are inserted behind the cleithral symphysis, with 2 robust rays each, and the medial ray is longer than the lateral ray. The gut is rotund, without loops, and is largely obscured laterally by large pectoral fins. It remains internal to the body and lacks the exterilium morphology of some other larval ophidiids (Fraser and Smith, 1974; Fahay and Nielsen, 2003; Okiyama, 2014). The anus is just anterior to the anal fin with no external extension. Dorsal, anal, and caudal fins are confluent. The dorsal- and anal-fin rays are approximately subequal in length to each other and along each fin. The teardrop-shaped caudal fin is small, lacking procurrent rays, with 5 principal rays on the upper and 4 on lower hypural elements; the medial rays are the longest.

The following description is based on in-situ images of collected and uncollected specimens. Counting ventrally from the dorsalmost ray, the first 4 and fifteenth through twentieth pectoral-fin rays are markedly elongate, the former being extremely filamentous, elongated, and free from an intervening membrane. The third pectoral-fin ray is the longest, being 2 times or greater in length than the TL. The second, first, and fourth rays are the next longest, respectively. The first and fourth rays are comparable in length to the seventeenth and eighteenth rays, approaching 1.5 times in length of the non-elongate pectoral-fin rays. The eighteenth pectoral-fin ray is the longest among ventral elongate rays, followed by the seventeenth, nineteenth, sixteenth, fifteenth, and twentieth rays.

Live coloration of larval *Acanthonus myersi*

Hereafter, coloration is defined as non-melanistic chromatophores. The following descriptions are based on several in-situ photographs of the collected specimen and others (Figs. 2B, 4A–C). The body is broadly transparent, with areas of melanistic pigmentation present above the brain. The dorsal and anal fins are largely transparent. Coloration is predominantly in pectoral fins, with a gradient of color intensifying distally in all rays. The color is orange to yellow, but the intensity depends on the photographic techniques used and the lighting. The color in natural light is undocumented. All but the third pectoral-fin ray are most intensely colored distally. The elongate third ray has the greatest amount of coloration near the intense distal coloration of the first, second, and fourth pectoral-fin rays, which then fades to largely opaque for the remaining and majority of its length.

Pigmentation in ethanol of larval *Acanthonus myersi*

Fine, discrete melanophores are present on or posterior to the oral jaws. Melanophores are the most dense above the brain and surrounding rotund gut, with the largest melanophores anterior to and above the latter. The second and third pectoral-fin rays are densely pigmented with melanophores distally, but the rays are broken, and pigmentation across the entire rays is unknown. The fourth through fourteenth pectoral-fin rays and membrane retain a single row of melanophores along the distal margin (Fig. 4D). Pigmentation is absent from the distal margin of the elongate fifteenth through twentieth pectoral-fin rays.

Redescription of larval *Acanthonus armatus*

The original postflexion specimen described and illustrated by Okiyama (1981, 2014) has not been found. The specimen was collected at the surface offshore Iriomote Island, August 1980 by M. Okiyama. Measurements and counts: SL 47.6 mm; dorsal-fin rays 108; anal-fin rays 95; pectoral-fin rays 18; pelvic-fin rays 2; caudal-fin rays 8 (based on Okiyama, 2014:425; Table 2). Proportions in SL listed by Okiyama (2014): preanal length 20.0%; HL 15.0%; depth of pectoral-fin base 18% (Table 2).

The preflexion specimen (USNM 454556) was collected at depth offshore Kona, Hawaii, the night of 4 November 2021 by A. Deloach, N. Deloach, and D. Whitestone; photographed by D. Whitestone and S. Kovacs. Measurements and counts: SL 8.8 mm; TL 9.1 mm; dorsal-fin rays 100+; anal-fin rays 90+; pectoral-fin rays 18; pelvic-fin rays 2 (Fig. 5). Caudal rays and posterior dorsal- and anal-fin rays are indistinguishable. Proportions in SL: preanal length 20.0%; HL 20.1%; depth of pectoral-fin base 18.3%; pelvic rays, end of gut, anus, and anterior part of anal fin damaged; caudal peduncle absent; caudal fin not distinguished (Table 2). Proportions in HL: dorsal fin origin 112.2%; snout length 32.5%; eye diameter 31.2%; postorbital length 33.0%; upper jaw length 51.7%; lower jaw length 59.2%; lower jaw width 10.2% (Table 2).

The following description is based on USNM 454556. The differences illustrated by Okiyama (2014:425) are noted in parentheses below. The head is large, deeper than long, and the body tapers posteriorly to the end of the notochord. Maxilla and premaxilla are present, and the supramaxilla is indistinguishable. The distal end of the maxilla is dorsoventrally expanded with a straight posterior margin (concave). The posterior tip of the premaxilla nearly reaches the posterior margin of the maxilla. The premaxilla and dentary have small, distantly spaced teeth. A large rostral cartilage is attached to the ascending process of the premaxilla. The opercular-series has no spines (opercular

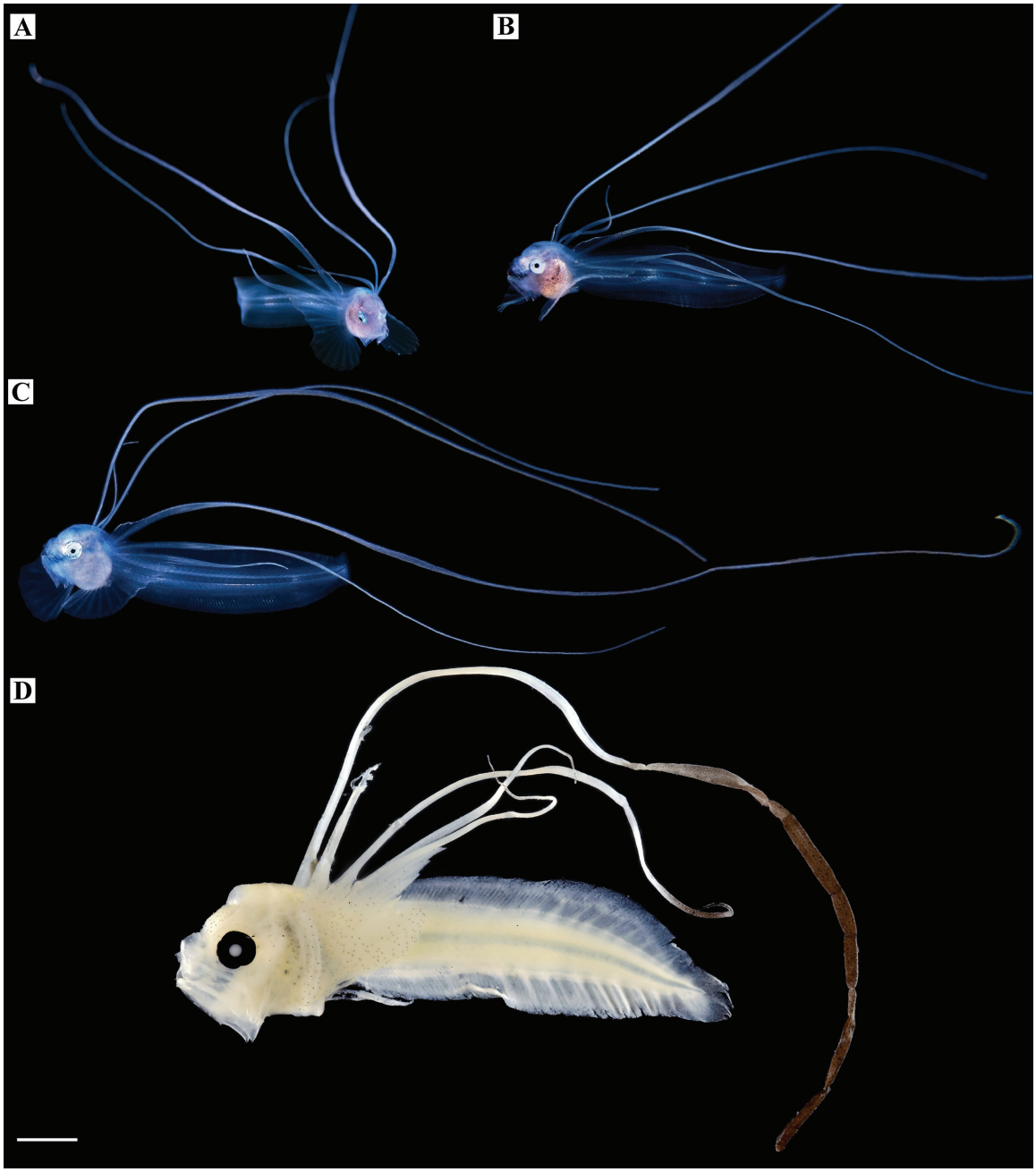

Figure 5

(**A–C**) Blackwater photos of a larval bony-eared assfish (*Acanthonus armatus*) (USNM 454556, 8.8 mm standard length) in the preflexion stage taken in the waters off Kona, Hawaii, on the night of 4 November 2021. Photo A © Steven Kovacs. Photos B and C © Dennis Whitestone. (**D**) Preserved specimen USNM 454556. Scale bar=1 mm.

and preopercular spines are present). At least 4 branchiostegals are evident (full complement 8). The body and head are scaleless. The pectoral fin is large and fan-like, with a broad base that is approximately the overall length of the head. There are 18 pectoral-fin rays on each side, but many rays were damaged. In-situ images of fixed specimen and uncollected specimens show pectoral-fin rays that were damaged and truncated during capture and subsequent preservation (compare Figs. 2A and 5A–C with 5D). Accordingly, the TL is not re-

Table 2

Comparison of larval traits among bony-eared assfish (*Acanthonus armatus*), spiny blind brotulid (*A. hextii*), and gargoyle cusk (*A. myersi*) based on in-situ larval photos and preserved larval and adult specimens. See the Material examined section for specimen information and museum catalog numbers. (SL=standard length; HL=head length.)

	Acanthonus armatus	*Acanthonus hextii*	*Acanthonus myersi*
Dorsal-fin rays	98–108	64–75	87–89
Apexes of second and third neural spines near dorsal margin of body	Not visible	Visible between posterior of neurocranium and first dorsal ray	Not visible
Pectoral-fin rays	16–19	18–19	19–20
Elongate and free pectoral-fin rays	3rd, 4th, 5th	Multiple but specific rays unknown	1st–4th; 15th–20th
Shape of elongate pectoral-fin rays	Broad, ribbon-like in large individuals	Unknown	Narrow, filamentous
Pectoral-fin membrane	Complete	Unknown	Distal membranes reduced
Pectoral-fin-membrane melanophores	Speckled	Absent	Single distal row
Pelvic-fin rays	2	2	2
Anal-fin rays	88–100	55–60	74–75
Precaudal vertebrae	9–10	11	12
Total vertebrae	60–65	53–54	49-52
Gut shape	Rotund	Rotund	Rotund
Caudal-fin rays on upper hypural plate	4	5	5
Caudal-fin rays on lower hypural plate	4	4	4
Head length in SL	15.0–20.1%	14.0%	20.5%
Pectoral-fin base depth in SL	18.0–18.3%	11.8%	15.7%
Medial pelvic-fin ray length in SL	Unknown	36.1%	28.9%
Lateral pelvic-fin ray length in SL	Unknown	36.1%	24.5%
Preanal length in SL	20.0%	30.2%	40.2%
Caudal-fin base depth in SL	Unknown	1.9%	3.3%
Dorsal-fin origin in HL	112.2%	128.8%	128.6%
Snout length in HL	32.5%	31.1%	27.2%
Eye diameter in HL	31.2%	24.3%	23.3%
Postorbital length in HL	33.0%	38.2%	46.4%
Upper jaw length in HL	51.7%	52.5%	53.2%
Lower jaw length in HL	59.2%	68.8%	50.9%

ported. The following description is based on in-situ images of collected and uncollected specimens: counting ventrally from the dorsalmost ray, the first 2 pectoral-fin rays are short, reduced, and bound to each other by a membrane throughout their length; the second is bound to the third through the length of the second (Figs. 2A, 5A–C). The third, fourth, and fifth rays are markedly elongate with a truncated membrane between them. The third pectoral-fin ray is the longest, 2× or more than the TL (almost equal to SL). The fourth and fifth rays are the next longest. Comparing live photos of preflexion (Fig. 5A–C) and postflexion (Fig. 2A) larvae, we observed the elongate rays becoming broad and ribbon-like through ontogeny. The broad tissue of the rays apparently dissipates or shrinks with fixation (see Okiyama, 2014:425). The pelvic-fin rays are inserted behind the cleithral symphysis. The rays were damaged in the fixed specimen, but live photos of this and other specimens show the rays to be moderately long and of nearly the same length (Fig. 2A). The gut is rotund, without loops, and is largely obscured laterally by large pectoral fins. It remains internal to the body and lacks exterilium morphology (see Fraser and Smith, 1974; Fahay and Nielsen, 2003; Okiyama, 2014). Posteriorly, the dorsal-fin, anal-fin, and notochord are confluent, with the former 2 becoming indistinguishable posteriorly (the caudal fin is teardrop-shaped, lacking procurrent rays, with 4 principal rays on the upper and 4 on the lower hypural elements; the medial rays are the longest). Dorsal- and anal-fin rays are approximately subequal in length to each other and along each fin.

Live coloration of larval *Acanthonus armatus*

The following description is based on several in-situ photographs of the collected specimen and others (Figs. 2A, 5A–C). The body is broadly transparent, with areas of melanistic pigmentation above the brain. The dorsal and

anal fins are largely transparent, lacking any noticeable coloration.

Pigmentation in ethanol of larval *Acanthonus armatus*

There are fine, discrete melanophores on or posterior to the oral jaws. The melanophores are most dense above the brain and surrounding the rotund gut, with the largest melanophores anterior to and above the latter. The membrane-bound pectoral-fin rays have speckled melanophores covering the fin. The third pectoral-fin ray is densely pigmented distally, becoming dark brown. A short band of dark pigmentation is present distally on the fourth pectoral ray (Fig. 5D).

Description of larval *Acanthonus hextii*

The postflexion specimen (USNM 439018) is from the eastern Indian Ocean (13°00′02″S, 117°53′09″E), 22 October 1977. Measurements and counts: SL 20.1 mm; TL 21.0 mm; dorsal-fin rays 72; anal-fin 54; pectoral-fin rays 18–19; pelvic-fin rays 2; caudal-fin rays 9 (Fig. 6, Table 2). Proportions in SL: preanal length 30.2%; HL 14.0%; depth of pectoral-fin base 11.8%; length of lateral and medial pelvic-fin rays 36.1%; caudal peduncle absent, narrowest caudal depth 1.9%; caudal-fin length 7.1% (Table 2). Proportions in HL: dorsal fin origin 128.8%; snout length 31.1%; eye diameter 24.3%; orbit diameter 28.2%; postorbital length 38.2%; upper jaw length 52.5%; lower jaw length 68.8%; lower jaw width 15.1% (Table 2).

The head is large, deeper than long, and the body tapers posteriorly to the end of the caudal fin. Maxilla and premaxilla are present, and the supramaxilla is indistinguishable. The distal end of the maxilla dorsoventrally expands with a concave posterior margin. The posterior tip of the premaxilla nearly reaches the posterior margin of the maxilla. Premaxilla and dentary have small, distantly spaced teeth. A large rostral cartilage is attached to the ascending process of the premaxilla. The opercle is thin with a posteriorly directed spine. The preopercle has 3 posteriorly directed spines, one on the vertical arm, one on the angle between the horizontal and vertical arms, and one on the horizontal arm (Fig. 6B). Five branchiostegals are evident (full complement 8). The body and head are scaleless. The pectoral fin is large and fan-like, with a broad base that is approximately the overall length of the head. The right pectoral fin has 18 rays and the left 19. The pectoral-fin membranes are robust but heavily damaged, and it is unclear if they are truncated or extend between the entire length of the rays. Counting ventrally from the dorsalmost ray, the second, third, sixth, eighth, and ninth through twelfth pectoral-fin rays are elongate, but all other rays were damaged (Fig. 6). Accordingly, the TL is not reported. The pelvic-fin rays are inserted behind the cleithral symphysis, 2 are approximately equal, robust rays. The gut is visible through the damaged pectoral fins and is rotund, without loops. It remains internal to the body and lacks exterilium morphology (see Fraser and Smith, 1974; Fahay and Nielsen, 2003; Okiyama, 2014). Apexes of the second and third vertebral neural arches are visible anterior to the first dorsal-fin ray, as in an adult. Posteriorly, the dorsal, anal, and caudal fins are confluent. The caudal fin is small, lacking procurrent rays, with 5 moderately elongate principal rays on the upper and 4 on the lower hypural elements. The dorsal- and anal-fin rays are approximately subequal in length to each other.

Pigmentation in ethanol of larval *Acanthonus hextii*

Specimen was housed in formalin for long period before transfer to ethanol. Few, discrete melanophores are on head and pectoral-fin bases (Fig. 6). Melanophores are most dense surrounding rotund gut, with the largest melanophores anterior to and above it. Dorsal- and anal fins have bands of brown coloration but lack discrete melanophores.

Discussion

Genera of the Ophidiidae and taxonomic changes

The integration of phylogenetic hypotheses and taxonomy allows for the generation of classifications that are reflective of current evolutionary understanding. Based on larval and adult morphological data, we hypothesize that the genera *Acanthonus, Tauredophidium,* and *Xyelacyba* form a monophyletic group within the Ophidiidae. This corroborates the hypotheses put forth by Cohen (1961) and Howes (1992). While our analysis of DNA data similarly recovers a close relationship between *A. armatus* and *A. myersi,* we recognize that our phylogeny is based on a limited sampling of one mitochondrial locus and includes only 2 of the 3 relevant taxa. Regardless, the morphological data supporting the monophyly of these 3 taxa is convincing, and the continued classification of these taxa as independent monotypic genera masks the current understanding of relationships among species. There have been relatively few assessments of the current classification of ophidiids above the genus level (e.g., Cohen and Nielsen, 1978; Howes, 1992; Nielsen et al., 1999; Møller et al., 2016), and 19 of the 51 genera (~37%) within the Ophidiidae are monotypic (Fricke et al., 2022). Placing the genera *Tauredophidium* and *Xyelacyba* in the synonymy of *Acanthonus* allows for the recognition of these taxa forming a clade. We list 4 larval

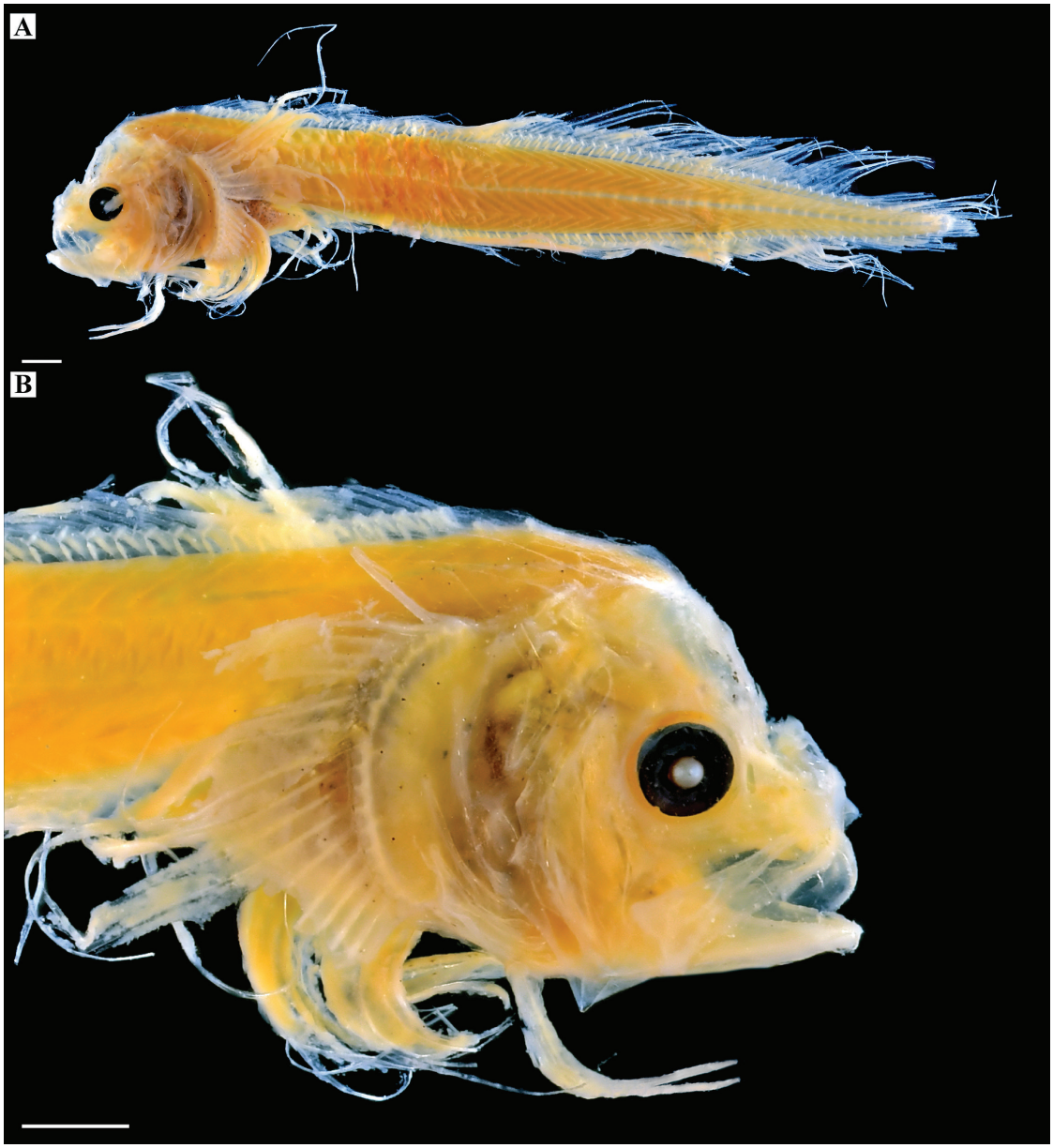

Figure 6

(**A**) Left side and (**B**) close-up of the right side of the head and pectoral fin of a larval spiny blind brotulid (*Acanthonus hextii*) (USNM 439018, 20.1 mm SL) in the postflexion stage. The specimen was collected from the eastern Indian Ocean on 22 October 1977. Scale bars=1 mm.

and 6 adult synapomorphic morphological characters that support the monophyly of *Acanthonus* below (Fig. 3B).

Comparison among larval thorny assfishes

While cusk-eel larvae are exceptionally diverse, no other larva was known to have pectoral-fin morphology like *A. armatus* prior to this study. The larval specimen of *A. myersi* from Florida (and other images of this form) and the specimen of *A. hextii* from the eastern Indian Ocean have characteristics similar to those described by Okiyama (2014), including large heads and fan-like pectoral fins. However, the morphology of the pectoral fins differs substantially among the 3 species of thorny assfishes, specifically in pectoral-fin ray elongation, structure and pigmentation, and extent of membrane between rays distally (Table 2). Larval *A. armatus* have the third, fourth, and fifth pectoral-fin rays markedly elon-

gate and free from membranes for the majority of their lengths, and the first 2 rays are much shorter and bound to each other by membranes throughout their lengths. Although the specimen used in Okiyama's (1981, 2014) descriptions has not been found, the illustration of the specimen, along with the specimen and photographs examined herein, shows only the third, fourth, and fifth rays elongate. The third ray is the longest, followed by the fourth and fifth rays. In larger specimens, the elongate rays appear broad and ribbon-like in live photographs (Fig. 2A), compared to the filamentous rays seen in the preflexion specimen collected from Hawaii. Although these rays likely broaden ontogenetically, they do not appear to remain broad through preservation, thus the illustration by Okiyama (2014:425) showing narrow elongate rays. In contrast, larval *A. myersi* have more elongate pectoral-fin rays (9), with the first 4 and fifteenth through twentieth rays being markedly elongate and free from membranes throughout most of their length (Table 2). These rays are thin and filamentous in in-situ images and preserved specimens. The pectoral fins of *A. hextii* are damaged in the specimen we identified, but it appears that at least the second, third, sixth, eighth, and ninth through twelfth pectoral-fin rays are elongate. This suggests that larval *A. hextii* may appear more similar to *A. myersi* in pectoral-fin morphology, with multiple rays elongate, as compared to the 3 elongate rays of *A. armatus* (Table 2). The pectoral-fin membranes of larval of *A. armatus* and *A. myersi* also differ strikingly, the former having each non-elongate ray connected by membrane along nearly the entire length of the ray, with only the distal tips slightly free. In contrast, larval *A. myersi* have this membrane truncated distally between all rays to various degrees (compare Fig. 2A with 2B, Table 2), with the truncation increasing ventrally along the fin. Due to pectoral-fin damage, it is unclear if the membrane is truncated or extends throughout the length of the rays in *A. hextii*. Differences in melanophores across the 3 taxa include discrete and scattered points on the pectoral fin in larval *A. armatus*, a single row of melanophores along the distal margin of the pectoral fin in larval *A. myersi*, and little to no pigmentation of the pectoral fin in larval *A. hextii* (Figs. 4–6). However, the specimen of *A. hextii* was preserved and stored in formalin for a long period prior to being transferred to ethanol, which may impact the pigmentation described in this study. There are also substantial differences in the live coloration of the pectoral-fin rays between larval *A. armatus* and *A. myersi* (Figs. 2, 4, 5) and differences in the length of the pelvic-fin rays among the 3 taxa (Fig. 3B, Table 2).

Despite the differences, the 3 larvae are strikingly similar and share 4 derived characters (Figs. 2, 3B, 4–6):

1. Pectoral-fin base broad.
2. Multiple pectoral-fin rays elongate and free.
3. Gut rotund.
4. Dense pigmentation surrounding the gut.

Three of these 4 characters are not currently known to occur in other cusk-eel larvae, with *Abyssobrotula* and *Dicrolene* having dense gut pigmentation dorsal and anterior to the gut (see Fahay, 2007:679, 689). Although the lengths of the pectoral rays are unknown for *A. hextii,* elongate rays approach or exceed the length of the body, and the longest pectoral-fin ray is the third ray in larval *A. armatus* and *A. myersi.* We expect that larval *A. hextii* have many elongate pectoral-fin rays, like *A. myersi,* and little pectoral pigmentation, like *A. armatus*. We hope that future sampling efforts throughout the Indo-West Pacific will capture larval specimens of *A. hextii,* as well as additional pre- and postflexion specimens of the remaining species of *Acanthonus,* and allow for subsequent phenotypic and genotypic comparisons to be made among these species.

Adult morphology and monophyly of *Acanthonus*

In 1992, Howes described the anatomy of adult *A. armatus* using 6 dissected 290–350 mm SL specimens. He described osteological, myological, and neurological traits, comparing those in *A. armatus* to other cusk-eels. While Howes (1992) was only able to examine radiographs of *A. hextii* and *A. myersi,* among others, he was able to hypothesize that these 3 taxa form a monophyletic group to the exclusion of all other members of the Ophidiidae. Considering the overall similarity among larval forms of *Acanthonus,* and previous hypotheses by Cohen (1961) and Howes (1992), we examined the adult morphology of the 3 species using a combination of cleared-and-stained and μCT-scanned specimens. We list 6 derived morphological characters (Fig. 3B, characters 5–10) that are diagnostic and support the monophyly of *Acanthonus*.

5. Opercular and preopercular spines with longitudinal keel (Fig. 7). Among the most prominent morphological traits of *A. armatus* are the elongate, robust spines associated with the opercular series (Figs. 1B and 7A). Both the opercle and preopercle have elongate, robust spines that approach or exceed the length of the premaxilla. Cohen (1961:291) called attention to the opercular spine of *A. myersi* as having a "lateral ridge with a deep groove on either side" (Figs. 1A and 7C). The lateral ridge, which we refer to as a longitudinal keel, is also present on the shorter preopercular spine of that species. This distinctive opercular and preopercular spine morphology also characterizes *A. armatus* and *A. hextii* (Figs. 1, B and C; 7, A and B), with the preopercle of *A. hextii* having an additional elongated, keeled spine on the vertical arm of the preopercle (Figs. 1C and 7B). Al-

though illustrated (see Alcock, 1892, plate 21; Nielsen, 1997, fig. 21), previous authors have not commented on the opercular and preopercular longitudinal keels in *A. armatus* and *A. hextii*. Opercular spines occur in other cusk-eels (e.g., *Dicrolene*; Fig. 7D), but their spines differ substantially from those of *Acanthonus*, most notably in being relatively flat, with little topographic relief (Fig. 3B).

6. Broad posterodorsal process of the quadrate embracing preopercle (Fig. 7). In his study on *A. armatus*, Howes (1992) highlighted a broad posterior process of the quadrate having a distinct articulation with the preopercle. This process, which is sometimes referred to as the posteroventral process (see Arratia and Schultze, 1991; Wiley and Johnson, 2010; Arratia, 2015), is laterally broad in *A. armatus*, with a distinct trough-like groove when viewed from the posterior aspect that embraces the anterior margin of the preopercular horizontal arm (Fig. 7A). Between the process and the preopercle, a thin band of connective tissue is also present, allowing the preopercle to articulate within the groove. The morphology of the process and articulation with the preopercle also characterizes *A. hextii* and *A. myersi* but not in the other taxa examined in our study (compare Fig. 7A–C with 7D). For example, *Dicrolene* has a narrow process, with a lamina present at the base of the trough (Fig. 7D). Howes (1992) noted that members of the genus *Lamprogrammus* have a similarly broad process that embraces the preopercle. While we agree that the process in *Lamprogrammus* is somewhat broad when compared to those of other genera of cusk-eels, the process does not embrace the preopercle both medially and laterally and does not contain connective tissue between the process and preopercle, as it does in *Acanthonus*.

7. Distantly spaced posterodorsal process and gap between preopercle and quadrate. Dorsal to the broadened posterodorsal process, a distinct gap is formed between the quadrate and anterior margin of the preopercle. The process is distantly spaced from the main body of the quadrate and lacks a bony lamina spanning the separation, allowing for a clear lateral view of the concomitantly separated symplectic (compare Fig. 7A–C with 7D). Across the cusk-eel taxa examined, the process is closely spaced to the main body of the quadrate and lacks a gap between the preopercle and quadrate dorsally (Fig. 3B).

8. Symplectic with the posterior spur (Figs. 7 and 8). Unlike the typical rod-like condition, the symplectic of *Acanthonus* has a posteriorly directed, acutely pointed spur (Fig. 7A–C). The acute point is not as apparent in the μCT scans (Fig. 7A–C) as it is in cleared-and-stained specimens (Fig. 8, D–G, J–M). This spur is easily visible laterally through the gap between the preopercle and quadrate described above. Such a spur has not been reported in cusk-eels, or percomorphs more broadly, and may be unique to this genus (Fig. 3B). We are unable to explain the representation of the symplectic in Howes' (1992, fig. 7) illustration of *A. armatus,* wherein he showed a rod-like symplectic lying between the metapterygoid and the preopercle, dorsally contacting the ventral arm of the hyomandibular but atypically short, not extending between the quadrate and posterodorsal process. Our examination shows the length of the symplectic is typically elongate in these 3 species, extending dorsally from the base of the quadrate to the ventral arm of the hyomandibular (Fig. 7).

9. Spine-extending and locking mechanism (Fig. 8). Cohen (1961) highlighted a spine-locking mechanism in the opercular-series of *A. myersi* (Fig. 8). When both the opercle and preopercle are rotated anteriorly, they lock in place, giving an "extremely fierce countenance when viewed head-on" (Cohen, 1961:291; Fig. 8A). He described 2 joints in the mechanism: "opercular spine forms a movable joint with the edge of the preopercle" and a movable joint between the anterior margin of the preopercle and "its anterior neighbor, presumably the hyomandibular" (Cohen, 1961:291). Our examination of the opercle and preopercle of *A. myersi* corroborates Cohen's observations that movable joints are associated with the anterior margins of both the opercle and preopercle and that these joints contribute to a spine-extending mechanism. However, the specific articulations and locations of the locking mechanism differ from those described by Cohen (1961). Aside from the prominent spine (see above), the opercle of *A. myersi* has 2 distinctive traits. Laterally, there is a knob-like process near the anterior margin of the opercle with a posterior notch (Fig. 8, D and E). Medially, there is a fossa with a large posterior flange reinforced by a keel of bone. This fossa articulates with the posterior arm of the hyomandibular (Fig. 8, F and G). When the opercle rotates forward, the lateral knob slides underneath the preopercle until its posterior notch embraces the vertical arm of the preopercle, locking the opercle in the forward position (compare Fig. 8, D and J, with 8, E and K). Simultaneously, the posterior arm of the hyomandibular slides from within the medial fossa to the posterior flange, rotating the opercle forward and extending the spine (compare Fig. 8, F and L, with 8, G and M). This distinctive opercular morphology and mechanism also characterize the opercula of *A. armatus* and *A. hextii* (Fig. 3B and Fig. 8, B and C, H–M). Although neither Alcock (1890) nor Howes (1992) noted locking mechanisms in *A. armatus* or *A. hextii*, Alcock (1890) mentioned that these bones can move. Howes (1992) highlighted an expanded *dilator operculi* in *A. armatus, A. hextii*, and *A. myersi,* and we corroborate his finding in *A. armatus*. The rotation of the opercle is generated by contraction of the expanded *dilator operculi,* which has 2 branches that insert on the dorsal margin of the opercle (Fig. 8, H and I). Two other muscles attach to the opercle, the

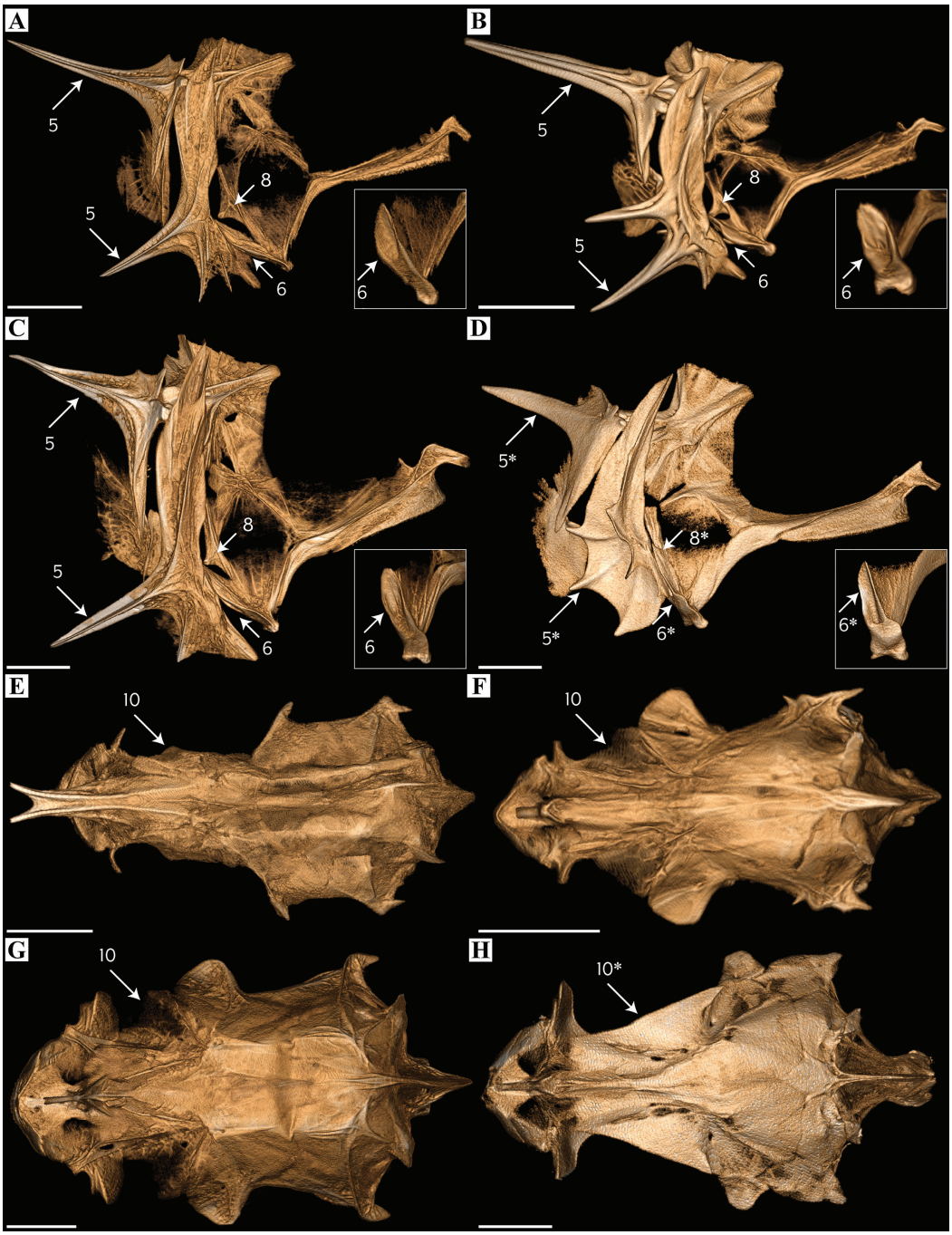

Figure 7

Micro-computed-tomography (µCT) scans of adult morphological characters in (A, E) bony-eared assfish (*Acanthonus armatus*) (UF 180163), (B, F) spiny blind brotulid (A. *hextii*) (BMNH 1992.2.4.3-4), (**C**, **G**) gargoyle cusk (*A. myersi*) (TCWC 10941.11), and (**D**, **H**) *Dicrolene introniger* (UW 4150) that support the monophyly of *Acanthonus*. Numbers correspond to the character numbers in the main text, and an asterisk (*) next to a number indicates the alternative character state. (**A–D**) Lateral views of right suspensorium and opercular series from segmented µCT scans. Cutouts below palatine arches are close-up images of the posterodorsal process in posterior view highlighting the width of the process. Characters: (5) keeled opercular and preopercular spines; (5*) flat spines of opercular series; (6) broad and distantly spaced posterodorsal process; (6*) narrow and closely spaced posterodorsal process; (8) posterior spur of symplectic; (8*) symplectic without posterior spur. (**E–H**) Dorsal view of isolated neurocranium from segmented µCT scans showing the (10) lateral flaring of frontal and the (10*) absence of frontal flaring. Scale bars=5 mm.

levator operculi inserting on the dorsal margin of the opercle and the *adductor operculi* inserting on the keel of the bone posterior to the medial fossa (Fig. 8, H and I). There is no muscular contribution to the forward rotation of the preopercle. The preopercular spines are extended as the opercular knob pushes the preopercle laterally, rotating the element within the broad posterodorsal process trough. We did not find a movable joint or locking mechanism between the preopercle and hyomandibular, as mentioned by Cohen (1961). Additionally, Howes (1992, fig. 27) described and illustrated a unique preopercular–opercular ligament (his "lpo") that stretches from the anteroventral margin of the opercle to the posterodorsal margin of the preopercle in *A. armatus, A. hextii,* and *A. myersi*. Given the passive rotation of the preopercle, we interpret the ligament to transmit force from the *adductor operculi,* which is attached to the opercle, to the preopercle when the muscle contracts to return the opercle to the resting position.

10. Laterally flared frontal (Fig. 7). Howes (1992, fig. 13A) illustrated a broad anterior and lateral extension of the frontal between the lateral ethmoid and sphenotic in *A. armatus* and noted a similar condition in *Glyptophidium* Alcock, 1889 (Alcock, 1889; Howes, 1992, fig. 14E). We corroborated this morphology in *A. armatus* (Fig. 7E) and found that a similarly flared frontal characterizes *A. hextii* and *A. myersi* (Fig. 7, F and G). The frontals in the latter 2 taxa are broader and extend a greater distance laterally than in *A. armatus*. Nonetheless, the frontal flaring in *Acanthonus* differs substantially from *Glyptophidium*, where the frontal is expanded throughout the lateral margin (see Howes, 1992, fig. 14E). Similar expansions of the frontal were not seen in any taxa outside of the examined *Acanthonus* (Fig. 3B).

Howes (1992) described additional characters supporting the monophyly of *A. armatus, A. hextii,* and *A. myersi* in soft tissue, including an expanded *levator arcus palatini,* which we could not observe in our specimens examined. However, the 4 larval (i.e., broad pectoral-fin bases, elongate pectoral-fin rays, rotund guts, and similar amounts of pigmentation on the head and surrounding the gut) and 6 adult morphological characters described above diagnose and strongly support the monophyly of *Acanthonus*. We anticipate that dense molecular sampling of these taxa will corroborate the monophyly of *Acanthonus* and encourage subsequent work that tests this hypothesis.

Sister-group relationship between *Acanthonus armatus* and *Acanthonus myersi*

Although Cohen (1961) and Howes (1992) hypothesized a close relationship among *A. armatus, A. hextii,* and *A. myersi,* explicit relationships among species of *Acanthonus* have remained uncertain. Howes (1992:130) emphasized that he could not resolve the relationships among the 3 taxa, as the anatomies of the latter 2 were "too imperfectly known." While the discovery of larval *A. hextii* and *A. myersi* strongly suggests that these taxa are closely related to *A. armatus,* the damage to the pectoral fins in the larval specimen of *A. hextii* prohibits the use of larval morphology in diagnosing relationships within *Acanthonus*. Despite this, we list 3 characters of the adult morphology (Fig. 3B, characters 11–13) that support a sister-group relationship between *A. armatus* and *A. myersi.*

11. Cancellous bone (Fig. 7). Cancellous or honeycomb-like bone is apparent throughout the skeleton in both *A. armatus* and *A. myersi,* including the opercular series, suspensorium, oral jaws, and vertebral elements (Figs. 7, A and C, 8D–M). However, *A. hextii* has smooth bone throughout these elements, with the exception of a cancellous subopercle (Figs. 3B and 7B).

12. Confluence of palatine and vomerine tooth plates. Although there are many similarities in the suspensoria of *Acanthonus* (Fig. 7A–C), there are differences in the orientation of the palatine among the 3 species. In both *A. armatus* and *A. myersi,* the palatine is closely applied to the vomer so that the narrow vomerine and palatine tooth plates are largely continuous when the mouth is closed. Howes (1992) highlighted this condition in *A. armatus* but did not mention that it also occurs in *A. myersi* (Fig. 3B). In *A. hextii*, a small gap is present between the palatine and vomer, and the tooth patches are not continuous when the mouth is closed.

13. Tripartite pharyngobranchial one (Fig. 9). *Acanthonus armatus* and *A. myersi* share an unusual tripartite pharyngobranchial one (Fig. 9, A and B). Pharyngobranchial one is typically a rod-like bone that suspends the branchial basket from the ventral margin of the braincase (Fig. 9C). In *A. armatus* and *A. myersi,* the first pharyngobranchial has 3 bony arms with cartilaginous caps; one arm is connected to epibranchial one, one arm directed laterally toward the ventral arm of the hyomandibular, and one arm directed toward the neurocranium (Fig. 9, A and B). In one specimen of *A. myersi*, a fourth arm is present (Fig. 9B); however, we treat this arm as anomalous as it was not found on the complementary pharyngobranchial in the same specimen or the specimen that was µCT-scanned. All other taxa examined, including *A. hextii*, have a typical rod-like first pharyngobranchial (Figs. 3B and 9C).

Based on characters 11–13, we hypothesize that *A. armatus* and *A. myersi* are sister taxa (Fig. 3B). We anticipate that dense molecular and morphological sampling of the 3 species of *Acanthonus* will similarly corroborate a sister-group relationship between *A. armatus* and *A. myersi* and encourage subsequent authors to test this hypothesis.

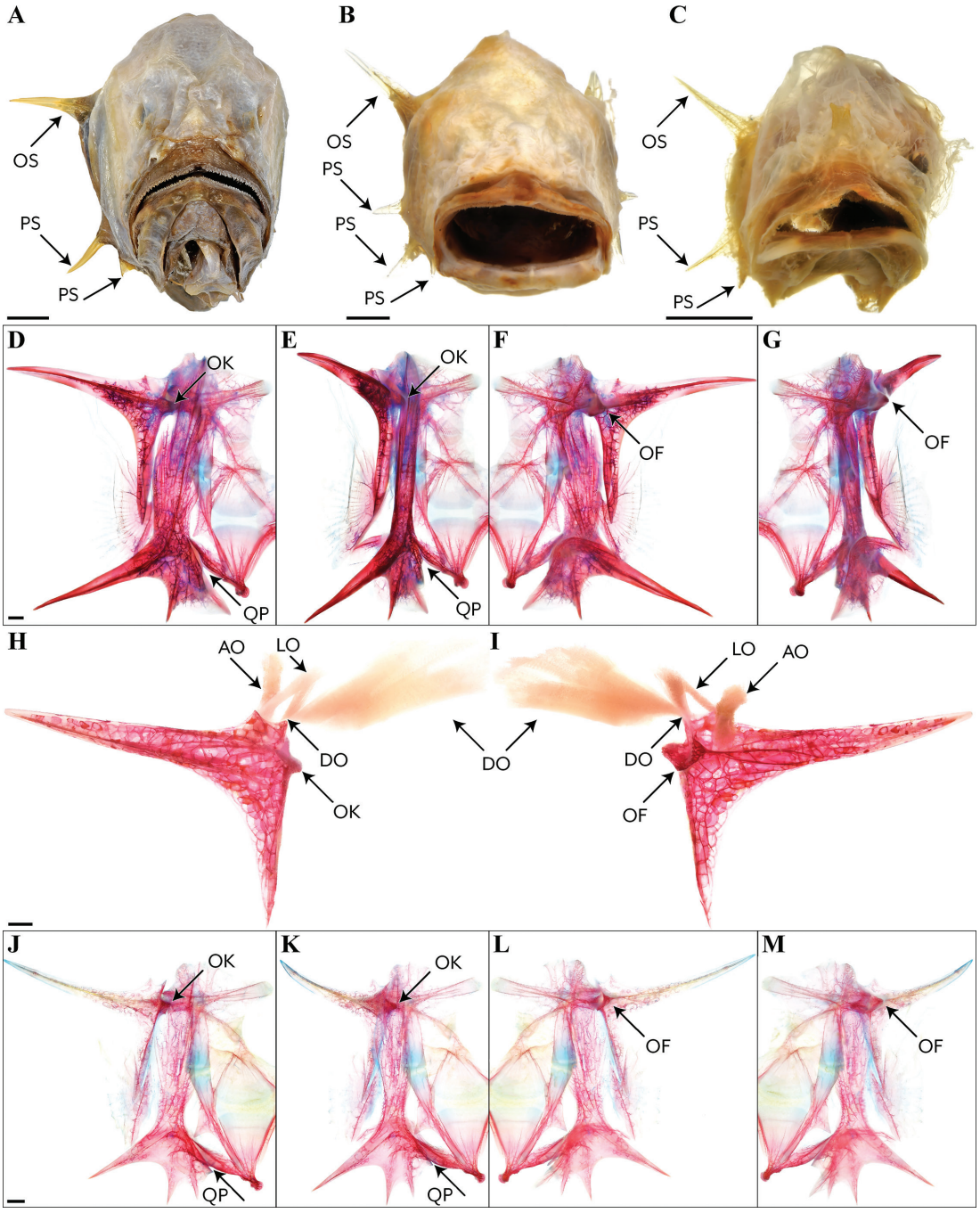

Figure 8

Images of the spine-extending and -locking mechanism (see morphological character 9) in 3 species of thorny assfishes (*Acanthonus*). A–C: Head-on images of (**A**) gargoyle cusk (*A. myersi*) (USNM 407808), (**B**) spiny blind brotulid (*A. hextii*) (BMNH 1992.2.4.3-4), and (**C**) bony-eared assfish (*A. armatus*) (UF 230821) that show the right opercle in locked position. Scale bars=5 mm. D, E: Lateral view of the right opercular series of *A. myersi* (USNM 407066) at (**D**) resting and (**E**) locked positions. F, G: Medial view of the right opercular series of *A. myersi* (USNM 407066) at (**F**) resting and (**G**) locked positions. H, I: (**H**) Lateral and (**I**) medial views of muscle insertions in the right opercle of *A. armatus* (UF 180163). J, K: Lateral view of the right opercular series of *A. armatus* (UF 180163) at (**J**) resting and (**K**) locked positions. L, M: Medial view of the right opercular series of *A. armatus* (UF 180163) at (**L**) resting and (**M**) locked positions. AO=*adductor operculi*; DO=*dilatator operculi*; LO=*levator operculi*; OK=opercular knob; OF=opercular medial flange; OS=opercular spine; PS=preopercular spine; QP=articulation between the quadrate and preopercle. Scale bars=1 mm.

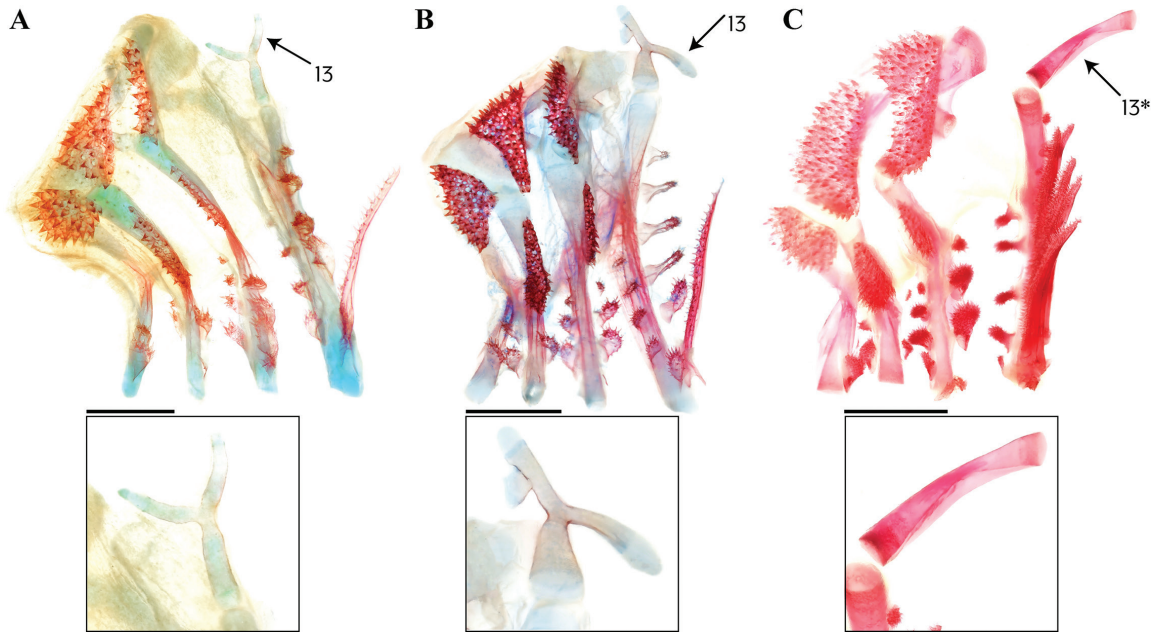

Figure 9

Images of pharyngobranchial one character (arrows) in (**A**) bony-eared assfish (*Acanthonus armatus*) (UF 180163), (**B**) gargoyle cusk (*A. myersi*) (USNM 407066), and (**C**) *Neobythites* sp. (USNM 395815) that support a sister-group relationship between *A. armatus* and *A. myersi*. The specimens of *A. armatus* and *A. myersi* have a tripartite pharyngobranchial one (13), while the specimen of *Neobythites* sp. has a rod-like pharyngobranchial one (13*). The number 13 corresponds to the character number in the main text. The cutouts below are close-up images of pharyngobranchial one. Scale bars=2 mm.

Conclusions

Blackwater divers and photographers have introduced new opportunities to learn more about the diversity of larval marine fishes (e.g., Nonaka et al., 2021). Integrating diver encounters, photographs, and preserved specimens with examination and sequencing of these larvae is critical to increasing our understanding of the natural history of marine fishes (e.g., Pastana et al., 2022; Girard et al., 2023b). The capture of larval *A. myersi* and *A. armatus* by these divers inspired subsequent comparisons of larval ophidiids, leading to the identification of a nearly 50-year-old museum specimen of larval *A. hextii*. We also want to highlight the importance of blackwater diving and photographs in understanding evolutionary relationships and the plethora of larval character data that can be observed in the photographs and collected specimens. In this study, in-situ photos and specimens captured by these divers allowed for the identification of several shared morphological traits among the larvae of these species and, along with examinations of the adult morphology, the generation of a hypothesis of relationships among them. We hope this study exemplifies how community science and collaboration can further our collective understanding of the evolution and natural history of marine fishes.

Material examined

Specimens are adult form unless otherwise denoted as "Larva-" preceding specimen preparation type. Specimens examined as prepared cleared-and-stained specimens are denoted as "-CS"; specimens examined as whole ethanol specimens are denoted as "-ET" with an "*" indicating one specimen was µCT scanned. Associated media identifiers for µCT image stacks available through MorphoSource are listed in brackets following the preparation types.

Acanthonus armatus: UF 113613 (1 ET); UF 179775 (1 ET); UF 179776 (1 ET); UF 179779 (2 ET); UF 180163 (2 CS; 4 ET*) [434905]; UF 230821 (4 ET); USNM 454556 (1 Larva-ET)
Acanthonus hextii: BMNH 1890.11.28.38 (1 ET); BMNH 1992.2.4.3-4 (2 ET*) [434911]; USNM 439018 (1 Larva-ET).
Acanthonus myersi: TCWC 10941.11 (1 ET*)

[59100; 59105]; USNM 407066 (1 CS); 407808 (1 ET); USNM 464023 (1 Larva-ET)
Brosmophyciops sp.: USNM 395812 (1 CS)
Brotula multibarbata: UW 14001 (1 ET*) [75512]
Dicrolene intronigra: USNM 395798 (1 CS); UW 4150 (1 ET*) [73383]
Dicrolene kanazawai: USNM 215302 (1 CS)
Glyptophidium sp.: USNM 395810 (1 CS)
Lamprogrammus exutus: USNM 296853 (1 CS; 7 ET); USNM 395809 (1 CS)
Lamprogrammus niger: UW 47373 (1 ET*) [75498]
Neobythites sp.: USNM 395815 (1 CS)
Sirembo sp.: USNM 395814 (1 CS)
Sirembo imberbis: UF 118246 (1 ET*) [160018; 160040]

Acknowledgments

We thank the organizers of this volume for inviting us to participate; B. Mundy (Ocean Research Explorations) and K. Tang (University of Michigan, Flint) for helpful discussions about ophidiids; blackwater divers A. Deloach, N. Deloach, S. Kovacs, J. Milisen, and D. Whitestone for capturing larval specimens, providing behavioral accounts, and allowing us to use some of their stunning photographs in this publication; R. Collins, D. Devers, L. Ianniello, and J. Milisen for their continued enthusiasm, useful discussions, and contributions to the USNM collections; J. Hill and S. Whittaker (NMNH) for assistance with µCT scanning; M. Pastana for assistance with myology; J. Maclaine (BMNH), J. Kojima (Marine Ecology Research Institute), N. Schnell (MNHN), A. Reft and L. Willis (National Systematics Laboratory, National Oceanic and Atmospheric Administration), K. Matsuura, M. Nakae, G. Shinohara (NSMT), R. Robbins (UF), and K. Murphy, D. Pitassy, and S. Raredon (USNM) for providing data, images, support, and/or access to specimens in their care; and K. Conway (TCWC), Z. Randall and E. Stanley (UF), A. Summers (UW), and the NSF-funded oVert project for making µCT scans publicly available through MorphoSource. This study was funded in part by the Herbert R. and Evelyn Axelrod Endowment for Systematic Ichthyology at NMNH and the NMNH Office of the Associate Director for Science. All DNA extractions and sequencing were conducted at the NMNH Laboratories of Analytical Biology. Lastly, a special thanks to our good friends and colleagues, G. Moser and M. Okiyama, who inspired and led us into the extraordinary world of larval fishes. We miss them and regret that we cannot continue to share with them the discoveries that come from the new arena of blackwater diving and photography. As indicated in our epigraph, we had shared many of the images with Geoff for the past several years, and he always expressed his amazement and fascination with them. G. D. Johnson and A. Nonaka benefited greatly from the many discussions they had with him during that time.

Literature cited

Alcock, A.
1889. Natural history notes from H.M. Indian Marine Survey Steamer 'Investigator,' Commander Alfred Carpenter, R.N., D.S.O., commanding.—No. 13. On the bathybial fishes of the Bay of Bengal and neighbouring waters, obtained during the seasons 1885–1889. Ann. Mag. Nat. Hist. Zool. Bot. Geol. 4:376–399. https://doi.org/10.1080/00222938909460547
1890. Natural history notes from H.M. Indian Marine Survey Steamer 'Investigator,' Commander R. F. Hoskyn, R. N., commanding.—No. 16. On the bathybial fishes collected in the Bay of Bengal during the season 1889–90. Ann. Mag. Nat. Hist. Ser. 6:197–222. https://doi.org/10.1080/00222939008694027
1892. Illustrations of the zoology of H. M. Indian Marine Survey Steamer Investigator Part 1. Fishes, plates 1–7. Supt. Gov. Print., Calcutta, India.

Arratia, G.
2015. Complexities of early Teleostei and the evolution of particular morphological structures through time. Copeia 103:999–1025. https://doi.org/10.1643/CG-14-184

Arratia, G., and H.-P. Schultze.
1991. Palatoquadrate and its ossifications: development and homology within osteichthyans. J. Morphol. 208:1–81. https://doi.org/10.1002/jmor.1052080102

Baldwin, C. C., and G. D. Johnson.
1995. A larva of the Atlantic flashlight fish, *Kryptophanaron alfredi* (Beryciformes: Anomalopidae), with a comparison of beryciform and stephanoberyciform larvae. Bull. Mar. Sci. 56:1–24.
2014. Connectivity across the Caribbean Sea: DNA barcoding and morphology unite an enigmatic fish larva from the Florida Straits with a new species of sea bass from deep reefs off Curaçao. PLoS ONE 9(5):e97661. https://doi.org/10.1371/journal.pone.0097661

Baldwin, C. C., G. D. Johnson, and P. L. Colin.
1991. Larvae of *Diploprion bifasciatum*, *Belonoperca chabanaudi* and *Grammistes sexlineatus* (Serranidae: Epinephelinae) with a comparison of known larvae of other Epinephelines. Bull. Mar. Sci. 48:67–93.

Baldwin, C. C., J. H. Mounts, D. G. Smith, and L. A. Weigt.
2009. Genetic identification and color descriptions of early life-history stages of Belizean *Phaeoptyx* and *Astrapogon* (Teleostei: Apogonidae) with comments on identification of adult *Phaeoptyx*. Zootaxa 2008:1–22. https://doi.org/10.11646/zootaxa.2008.1.1

Bleeker, P.
1857. Vierde bijdrage tot de kennis der ichthyologische fauna van Japan. Acta Soc. R. Sci. Indo-Neêrlandicae 3(art. 10), 46 p.

Chang, C.-H., K.-T. Shao, H.-Y. Lin, Y.-C. Chiu, M.-Y. Lee, S.-H. Liu, and P.-L Lin.
2017. DNA barcodes of the native ray-finned fishes in Taiwan. Mol. Ecol. Resour. 17:796–805. https://doi.org/10.1111/1755-0998.12601

Chernomor, O., A. von Haeseler, and B. Q. Minh.
2016. Terrace aware data structure for phylogenomic infer-

ence from supermatrices. Syst. Biol. 65:997–1008. https://doi.org/10.1093/sysbio/syw037

Cohen, D. M.
1961. A new genus and species of deepwater ophidioid fish from the Gulf of Mexico. Copeia 1961:288–292. https://doi.org/10.2307/1439802

Cohen, D. M., and J. G. Nielsen.
1978. Guide to the identification of genera of the fish order Ophidiiformes with a tentative classification of the order. NOAA Tech. Rep. NMFS Circ. 417, 72 p.

Fahay, M. P.
2007. Early stages of fishes in the western North Atlantic Ocean (Davis Strait, Southern Greenland and Flemish Cap to Cape Hatteras). Volume 1: Acipenseriformes through Syngnathiformes, 931 p. NAFO, Dartmouth, Canada.

Fahay, M. P., and J. G. Nielsen.
2003. Ontogenetic evidence supporting a relationship between *Brotulotaenia* and *Lamprogrammus* (Ophidiiformes: Ophidiidae) based on the morphology of exterilium and rubaniform larvae. Ichthyol. Res. 50:209–220. https://doi.org/10.1007/s10228-003-0159-5

Fedorov, A., R. Beichel, J. Kalpathy-Cramer, J. Finet, J.-C. Fillion-Robin, S. Pujol, C. Bauer, D. Jennings, F. Fennessy, M. Sonka, et al.
2012. 3D Slicer as an image computing platform for the Quantitative Imaging Network. Magn. Reson. Imaging 30:1323–1341. https://doi.org/10.1016/j.mri.2012.05.001

Fraser, T. H., and M. M. Smith.
1974. An exterilium larval fish from South Africa with comments on its classification. Copeia 1974:886–892. https://doi.org/10.2307/1442587

Fricke, R., W. N. Eschmeyer, and R. Van der Laan (eds.).
2022. Eschmeyer's Catalog of Fishes: genera, species, references. [Available from http://researcharchive.calacademy.org/research/ichthyology/catalog/fishcatmain.asp, accessed March 2022.]

Gerringer, M. E., T. D. Linley, and J. G. Nielsen.
2021. Revision of the depth record of bony fishes with notes on hadal snailfishes (Liparidae, Scorpaeniformes) and cusk eels (Ophidiidae, Ophidiiformes). Mar. Biol. 168:167. https://doi.org/10.1007/s00227-021-03950-8

Gill, T.
1861. Notes on some genera of fishes of the western coast of North America. Proc. Acad. Nat. Sci. Phila. 13:164–168.
1863. Deecriptions [*sic*] of the genera of gadoid and brotuloid fishes of western North America. Proc. Acad. Nat. Sci. Phila. 15:242–254.

Girard, M. G., M. P. Davis, and W. L. Smith.
2020. The phylogeny of carangiform fishes: morphological and genomic investigations of a new fish clade. Copeia 108:265–298. https://doi.org/10.1643/ci-19-320

Girard, M. G., M. P. Davis, Tan H. H., D. J. Wedd, P. Chakrabarty, W. B. Ludt, A. P. Summers, and W. L. Smith.
2022. Phylogenetics of archerfishes (Toxotidae) and evolution of the toxotid shooting apparatus. Integr. Org. Biol. 4:obac013. https://doi.org/10.1093/iob/obac013

Girard, M. G., H. J. Carter, and G. D. Johnson.
2023a. New species of *Monomitopus* (Ophidiidae) from Hawai'i, with description of a larval coiling behavior. Zootaxa 5330(2):265–279. https://doi.org/10.11646/zootaxa.5330.2.5

Girard, M. G., B. C. Mundy, A. Nonaka, and G. D. Johnson.
2023b. Cusk-eel confusion: revisions of larval *Luciobrotula* and *Pycnocraspedum* and re-descriptions of two bythitid larvae (Ophidiiformes). Ichthyol. Res. 70:474–489. https://doi.org/10.1007/s10228-023-00906-4

Goode, G. B., and T. H. Bean.
1883. Reports on the results of dredging under the supervision of Alexander Agassiz, on the East Coast of the United States, during the summer of 1880, by the U. S. Coast Survey Steamer "Blake," Commander J. R. Bartlett, U. S. N., commanding. Bull. Mus. Comp. Zool. 10:183–226.

Günther, A.
1878. Preliminary notices of deep-sea fishes collected during the Voyage of H. M. S. 'Challenger'. Ann. Mag. Nat. Hist. 2(7):17–28.
1887. Report on the deep-sea fishes collected by H. M. S. Challenger during the years 1873–76. Report on the Scientific Results of the Voyage of H. M. S. Challenger, vol. 22, part 57, 268 p. London.

Howes, G. J.
1992. Notes on the anatomy and classification of ophidiiform fishes with particular reference to the abyssal genus *Acanthonus* Günther, 1878. Bull. Br. Mus. Nat. Hist. (Zool.) 58:96–131.

Jenkins, J. A., H. L. Bart Jr., P. R. Bowser, J. R. MacMillan, J. G. Nickum, J. D. Rose, P. W. Sorensen, G. W. Whitledge, J. W. Rachlin, and B. E. Warkentine.
2014. Guidelines for the use of fishes in research, 90 p. Am. Fish. Soc., Bethesda, MD.

Johnson, G. D.
1984. Percoidei: development and relationships. *In* Ontogeny and systematics of fishes, based on an international symposium dedicated to the memory of Elbert Halvor Ahlstrom, August 15–18, 1983, La Jolla, California (H. G. Moser, W. J. Richards, D. M. Cohen, M. P. Fahay, A. W. Kendall Jr., and S. L. Richardson, eds.), p. 464–498. Spec. Publ. 1. Am. Soc. Ichthyol. Herpetol., Lawrence, KS.
1988. *Niphon spinosus*, a primitive epinepheline serranid: corroborative evidence from the larvae. Jpn. J. Ichthyol. 35:7–18.

Johnson, G. D., and B. B. Washington.
1987. Larvae of the Moorish Idol, *Zanclus cornutus*, including a comparison with other larval acanthuroids. Bull. Mar. Sci. 40:494–511.

Johnson, G. D., J. R. Paxton, T. T. Sutton, T. P. Satoh, T. Sado, M. Nishida, and M. Miya.
2009. Deep-sea mystery solved: astonishing larval transformations and extreme sexual dimorphism unite three fish families. Biol. Lett. 5:235–239. https://doi.org/10.1098/rsbl.2008.0722

Johnson, R. K., and E. Bertelsen.
1991. The fishes of the family Giganturidae: systematics, development, distribution and aspects of biology. Dana Rep. 91:1–45.

Kalyaanamoorthy, S., B. Q. Minh, T. K. F. Wong, A. von Haeseler, and L. S. Jermiin.
2017. ModelFinder: fast model selection for accurate phylogenetic estimates. Nat. Methods 14:587–589. https://doi.org/10.1038/nmeth.4285

Katoh, K., and D. M. Standley.
2013. MAFFT multiple sequence alignment software version 7: improvements in performance and usability. Mol. Biol. Evol. 30:772–780. https://doi.org/10.1093/molbev/mst010

Kawaguchi, K., and H. G. Moser.
1984. Stomiatoidea: development. *In* Ontogeny and systematics of fishes, based on an international symposium dedicated to the memory of Elbert Halvor Ahlstrom, August 15–18, 1983, La Jolla, California (H. G. Moser, W. J. Richards, D. M. Cohen, M. P. Fahay, A. W. Kendall Jr., and S.

L. Richardson, eds.), p. 169–181. Spec. Publ. 1. Am. Soc. Ichthyol. Herpetol., Lawrence, KS.

Kearse, M., R. Moir, A. Wilson, S. Stones-Havas, M. Cheung, S. Sturrock, S. Buxton, A. Cooper, S. Markowitz, C. Duran, et al.
2012. Geneious Basic: an integrated and extendable desktop software platform for the organization and analysis of sequence data. Bioinformatics 28:1647–1649. https://doi.org/10.1093/bioinformatics/bts199

Kenchington, E. L., S. M. Baillie, T. J. Kenchington, and P. Bentzen.
2017. Barcoding Atlantic Canada's mesopelagic and upper bathypelagic marine fishes. PLoS ONE 12(9):e0185173. https://doi.org/10.1371/journal.pone.0185173

Leis, J. M.
2015. Taxonomy and systematics of larval Indo-Pacific fishes: a review of progress since 1981. Ichthyol. Res. 62:9–28. https://doi.org/10.1007/s10228-014-0426-7

Leis, J. M., and B. M. Carson-Ewart (eds.).
2000. The larvae of Indo-Pacific coastal fishes: an identification guide to marine fish larvae, vol. 2, 850 p. Brill, Leiden, Netherlands.

Minh, B. Q., H. A. Schmidt, O. Chernomor, D. Schrempf, M. D. Woodhams, A. von Haeseler, and R. Lanfear.
2020. IQ-TREE 2: new models and efficient methods for phylogenetic inference in the genomic era. Mol. Biol. Evol. 37:1530–1534. https://doi.org/10.1093/molbev/msaa015

Møller, P. R., S. W. Knudsen, W. Schwarzhans, and J. G. Nielsen.
2016. A new classification of viviparous brotulas (Bythitidae) – with family status for Dinematichthyidae – based on molecular, morphological and fossil data. Mol. Phylogenet. Evol. 100:391–408. https://doi.org/10.1016/j.ympev.2016.04.008

Moser, H. G.
1981. Morphological and functional aspects of marine fish larvae. *In* Marine fish larvae: morphology, ecology, and relation to fisheries (R. Lasker, ed.), p. 89–131. Wash. Sea Grant Program, Seattle, WA.
1996. The early stages of fishes in the California Current region. CalCOFI Atlas 33, 1505 p.

Moser, H. G, W. J. Richards, D. M. Cohen, M. P. Fahay, A. W. Kendall Jr., and S. L. Richardson (eds.).
1984. Ontogeny and systematics of fishes, based on an international symposium dedicated to the memory of Elbert Halvor Ahlstrom, August 15–18, 1983, La Jolla, California. Spec. Publ. 1. Am. Soc. Ichthyol. Herpetol., Lawrence, KS.

Nielsen, J. G.
1997. Deepwater ophidiiform fishes from off New Caledonia with six new species. No. 4, *In* Résultats des Campagnes MUSORSTOM, vol. 17 (B. Séret, ed.), p. 51–82. Mém. Mus. Natl. Hist. Nat. 174, Paris.

Nielsen, J. G., D. M. Cohen, D. F. Markle, and C. R. Robins.
1999. FAO species catalogue. Volume 18. Ophidiiform fishes of the world (Order Ophidiiformes). An annotated and illustrated catalogue of pearlfishes, cusk-eels, brotulas and other ophidiiform fishes known to date. FAO Fish. Synop. 125, 178 p. FAO, Rome.

Nonaka, A., J. W. Milisen, B. C. Mundy, and G. D. Johnson.
2021. Blackwater diving: an exciting window into the planktonic arena and its potential to enhance the quality of larval fish collections. Ichthyol. Herpetol. 109:138–156. https://doi.org/10.1643/i2019318

Okiyama, M.
1981. Manuals for the larval fish taxonomy (8), Ophidiiformes and "Incertae sedis". Aquabiology 3:258–262. [In Japanese.]

Okiyama, M. (ed.).
1988. An atlas of early stage fishes in Japan, 1154 p. Tokai Univ. Press, Tokyo, Japan. [In Japanese.]
2014. An atlas of early stage fishes in Japan, 2nd ed., 1896 p. Tokai Univ. Press, Hadano, Japan. [In Japanese.]

Okiyama, M., and M. Yamaguchi.
2004. A new type of exterilium larva referable to *Leptobrotula* (Ophidiiformes: Ophidiidae: Neobythitinae) from tropical Indo-West Pacific. Ichthyol. Res. 51:77–80. https://doi.org/10.1007/s10228-003-0189-z

Parr, A. E.
1933. Deepsea Berycomorphi and Percomorphi from the waters around the Bahama and Bermuda islands. Bull. Bingham Oceanogr. Coll. 3(art. 6), 51 p.

Pastana, M. N. L., M. G. Girard, M. I. Bartick, and G. D. Johnson
2022. A novel association between larval and juvenile *Erythrocles schlegelii* (Teleostei: Emmelichthyidae) and pelagic tunicates. Ichthyol. Herpetol. 110:675–679. https://doi.org/10.1643/i2022008

Pietsch, T. W.
1984. Lophiiformes: development and relationships. *In* Ontogeny and systematics of fishes, based on an international symposium dedicated to the memory of Elbert Halvor Ahlstrom, August 15–18, 1983, La Jolla, California (H. G. Moser, W. J. Richards, D. M. Cohen, M. P. Fahay, A. W. Kendall Jr., and S. L. Richardson, eds.), p. 320–325. Spec. Publ. 1. Am. Soc. Ichthyol. Herpetol., Lawrence, KS.

Potthoff, T.
1984. Clearing and staining techniques. *In* Ontogeny and systematics of fishes, based on an international symposium dedicated to the memory of Elbert Halvor Ahlstrom, August 15–18, 1983, La Jolla, California (H. G. Moser, W. J. Richards, D. M. Cohen, M. P. Fahay, A. W. Kendall Jr., and S. L. Richardson, eds.), p. 35–37. Spec. Publ. 1. Am. Soc. Ichthyol. Herpetol., Lawrence, KS.

Richards, W. J. (ed.).
2006. Early stages of Atlantic fishes: an identification guide for the western central north Atlantic, 1312 p. Taylor and Francis, Boca Raton, FL.

Robertson, D. R., A. Angulo, C. C. Baldwin, D. Pitassy, A. Driskell, L. Weigt, and I. J. F. Navarro.
2017. Deep-water bony fishes collected by the B/O Miguel Oliver on the shelf edge of Pacific Central America: an annotated, illustrated and DNA-barcoded checklist. Zootaxa 4348:1–125. https://doi.org/10.11646/zootaxa.4348.1.1

Rolfe, S., S. Pieper, A. Porto, K. Diamond, J. Winchester, S. Shan, H. Kirveslahti, D. Boyer, A. Summers, and A. M. Maga.
2021. SlicerMorph: an open and extensible platform to retrieve, visualize and analyse 3D morphology. Methods Ecol. Evol. 12:1816–1825. https://doi.org/10.1111/2041-210X.13669

Sabaj, M. H.
2020. Codes for natural history collections in ichthyology and herpetology. Copeia 108:593–669. https://doi.org/10.1643/ASIHCODONS2020

Tyler, J. C., G. D. Johnson, I. Nakamura, and B. B. Collette.
1989. Morphology of *Luvarus imperialis* (Luvaridae) with a phylogenetic analysis of the Acanthuroidei (Pisces). Smithson. Contrib. Zool. 485, 78 p.

Weigt, L. A., A. C. Driskell, C. C. Baldwin, and A. Ormos.
2012. DNA barcoding fishes. *In* DNA barcodes: methods and protocols (W. J. Kress and D. L. Erickson, eds.), p. 109–126. Humana Press, Totowa, NJ.

Weihs, D., and H. G. Moser.
1981. Stalked eyes as an adaptation towards more efficient foraging in marine fish larvae. Bull. Mar. Sci. 31:31–36.
Whitley, G. P.
1941. Ichthyological notes and illustrations. Aust. Zool. 10:1–50.
Wiley, E. O., and G. D. Johnson.
2010. A teleost classification based on monophyletic groups. *In* Origin and phylogenetic interrelationships of Teleosts (J. S. Nelson, H.-P. Schultze, and M. V. H. Wilson, eds.), p. 123–182. Verlag Dr. F. Pfeil, München, Germany.
Winterbottom, R.
1993. Myological evidence for the phylogeny of recent genera of surgeonfishes (Percomorpha, Acanthuridae), with comments on the Acanthuroidei. Copeia 1993:21–39. https://doi.org/10.2307/1446292
Wood-Mason, J., and A. Alcock.
1891. Natural history notes from H.M. Indian Marine Survey Steamer 'Investigator,' Commander R. F. Hoskyn, R. N., commanding. Series 2, No. 1. On the results of deep-sea dredging during the season 1890–91. Ann. Mag. Nat. Hist. 8:16–34. https://doi.org/10.1080/00222939109460385

Published online 17 April 2024.

Cite as: Girard, M., A. Nonaka, C. C. Baldwin, and G. D. Johnson. 2024. Discovery and description of elaborate larval cusk-eels and the relationships among *Acanthonus, Tauredophidium,* and *Xyelacyba* (Teleostei: Ophidiidae). *In* Early Life History and Biology of Marine Fishes: Research inspired by the work of H Geoffrey Moser (J. M. Leis, W. Watson, B. C. Mundy, and P. Konstantinidis, guest eds.), p. 20-42. NOAA Professional Paper NMFS 24. https://doi.org/10.7755/PP.24.3